UNIVERSITY OF NAPLES FEDERICO II

PH.D. PROGRAM IN

CLINICAL AND EXPERIMENTAL MEDICINE

CURRICULUM IN TRANSLATIONAL PEDIATRIC SCIENCES

XXXVII Cycle
(Years 2021-2024)

Chairman: Prof. Francesco Beguinot

PH.D. THESIS

Novel oncogenic function of OFD1 in cholangiocarcinoma: insights into ciliary dysfunction and tumor growth

TUTOR

Prof. Brunella Franco

PH.D. STUDENT

Dr. Fabiola Piscopo

Table of Contents

Abstract

Cholangiocarcinoma (CCA) is a highly lethal malignancy arising from the transformation of cholangiocytes, the epithelial cells lining the biliary ducts. CCA is a rare and aggressive cancer comprising distinct subsets of biliary tumors different in histopathology and molecular alterations. Over recent decades, epidemiological trends have revealed increasing incidence and mortality rates worldwide. Diagnosis at late stages together with frequent emergence of chemoresistance contribute to the persistently poor prognosis of CCA patients.

The primary cilium is a solitary, non-motile, microtubule-based organelle extending from the surface of most epithelial cells. Defects in ciliary structure and/or function have been identified as etiological factors underlying ciliopathies, multisystem disorders characterized by extensive genetic heterogeneity and a wide spectrum of phenotypes affecting multiple organs. In addition to its structural role, the primary cilium functions as a critical signaling hub. Moreover, emerging evidence support its involvement in cancer development and progression.

In this work, we analyzed the transcriptome of a cohort of CCA patients, identifying the *OFD1* gene as one of the most upregulated transcripts. Through *in vitro* experiments, we demonstrated that OFD1 modulation significantly impacts cell proliferation and migration in both human healthy cholangiocytes and CCA cell lines by influencing several cancer-related signaling pathways. Preliminary data further suggested a correlation between OFD1 expression and patient prognosis. These findings propose ciliary genes, particularly *OFD1*, as potential biomarkers for improving the clinical management of CCA patients and provide novel insights into the role of primary cilia in cancer biology.

Introduction

1. Cholangiocarcinoma: introduction to current knowledge

1.1 Anatomical, histological and molecular classification of cholangiocarcinoma

Cholangiocarcinoma (CCA) encompasses a heterogenous group of primary neoplasms emerging from the biliary tree within and outside the liver. CCA represents the second most common primary hepatic malignancy after hepatocellular carcinoma (HCC), comprising approximately 15% of all primary liver cancers and ∼3% of all gastrointestinal tumors[1,2]. The classification of CCA has become a matter of intense discussion due to the considerable heterogeneity in terms of anatomic location, gross appearance, cells of origin and molecular alterations[3,4]. Regarding the anatomical site of origin, CCA can be classified into three main subtypes (Fig.1): intrahepatic CCA (iCCA), which originates from the bile ductules near the second-order bile ducts (segmental bile ducts); perihilar CCA (pCCA), which develops in the right and/or left hepatic duct or at their junction (the so-called perihilar bile ducts); and distal CCA (dCCA), which arises from the epithelium distal to the cystic duct insertion. pCCA and dCCA can be also collectively considered as extrahepatic CCA (eCCA), even if this classification is quite discouraged due to its lack of precise anatomical distinction[5,6]. Of note, there is an additional rare type of liver cancer, so called mixed HCC–CCA, that can be considered as an independent entity, sharing features of both iCCA and HCC[7].

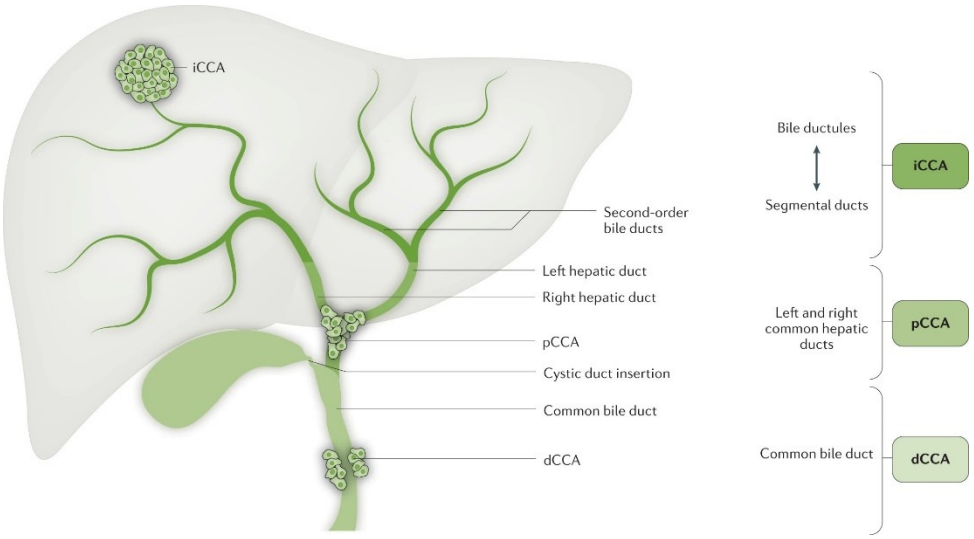

Figure 1. Anatomical classification of CCA.
On its anatomical origin, CCA is classified into three types: intrahepatic CCA (iCCA), perihilar CCA (pCCA), and distal CCA (dCCA). iCCA is found proximally in the peripheral regions of the second-order bile ducts within the liver parenchyma, pCCA arises in the right and/or left hepatic duct or at their confluence, while dCCA affects the common bile duct below the cystic duct insertion (adapted from Brindley *et al*., 2021).

iCCA can exhibit three distinct growth patterns (Fig. 2): mass-forming (MF-iCCA), periductal infiltrating (PI-iCCA), and intraductal growing (IG-iCCA), with MF-iCCA being the most common form[1,2,8]. For pCCA and dCCA, growth patterns similar to PI-iCCA or IG-iCCA can also occur. However, pCCA typically presents a nodular plus periductal infiltrating pattern, which is the most frequent form (>80%). MF-iCCA usually arises as a solid mass in peripheral small bile ducts within the hepatic parenchyma, while PI-iCCA and IG-iCCA are primarily found in larger intrahepatic bile ducts (segmental and area ducts). PI-iCCA tends to grow along the bile duct, causing biliary shrinkages and sometimes invading liver parenchyma, while IG-iCCA shows a papillary growth into the duct lumen. In addition, PI-iCCA is often preceded by preinvasive lesions. In contrast, preinvasive lesions for MF-iCCA are less frequent[9].

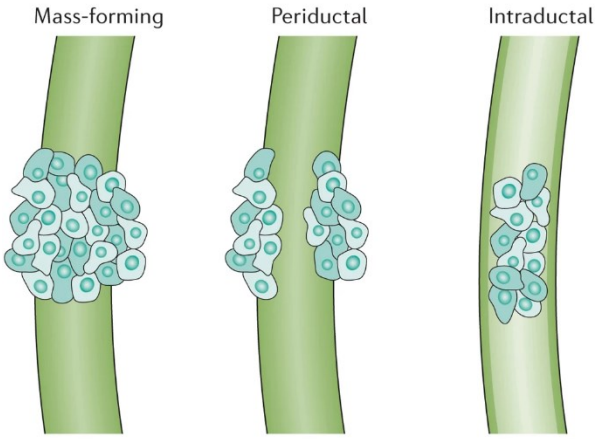

Figure 2. CCA classification according to gross appearance.
Cholangiocarcinoma (CCA) typically presents with three primary growth patterns: mass-forming, periductal-infiltrating, and intraductal-growing. Mass-forming CCA appears as a solid mass within the hepatic parenchyma. Periductal-infiltrating iCCA grows within the duct wall, extending longitudinally along its length. Intraductal-growing CCA manifests as a polypoid or papillary tumor that grows into the duct lumen (adapted from Banales *et al*., 2016).

Histologically, it has been established that pCCA and dCCA are generally mucin-producing adenocarcinomas or papillary tumors, while iCCA has more histological diversity (Fig. 3). In fact, iCCA includes subtypes, such as cholangiolocarcinoma (CLC) and two rare variants: small bile duct-iCCA and large bile duct-iCCA[10]. Small bile duct-iCCA and CLC subtypes originate in the smaller intrahepatic bile ducts and ductules, likely from hepatic stem or progenitor cells (HpSCs) and cuboidal cholangiocytes, which form the surface epithelium in these areas. Small bile duct-iCCA typically presents as a small tubular or acinar adenocarcinoma, infiltrating liver tissue with no or minimal mucin production. These iCCA subtypes usually develop on the background of chronic liver conditions, like viral hepatitis and cirrhosis, which activate HpSCs[11].

By contrast, large bile duct-iCCA, as well as pCCA and dCCA, originate in large ducts lined by columnar mucin-producing cholangiocytes or peribiliary gland cells, which may also give rise to precursor lesions such as intraductal papillary neoplasms. These subtypes are commonly associated with chronic inflammatory conditions, including primary sclerosing cholangitis (PSC) and liver fluke infections, where inflammation promotes cell proliferation and metaplasia within the ducts, leading to dysplasia and potentially predisposes to malignancy[1,6].

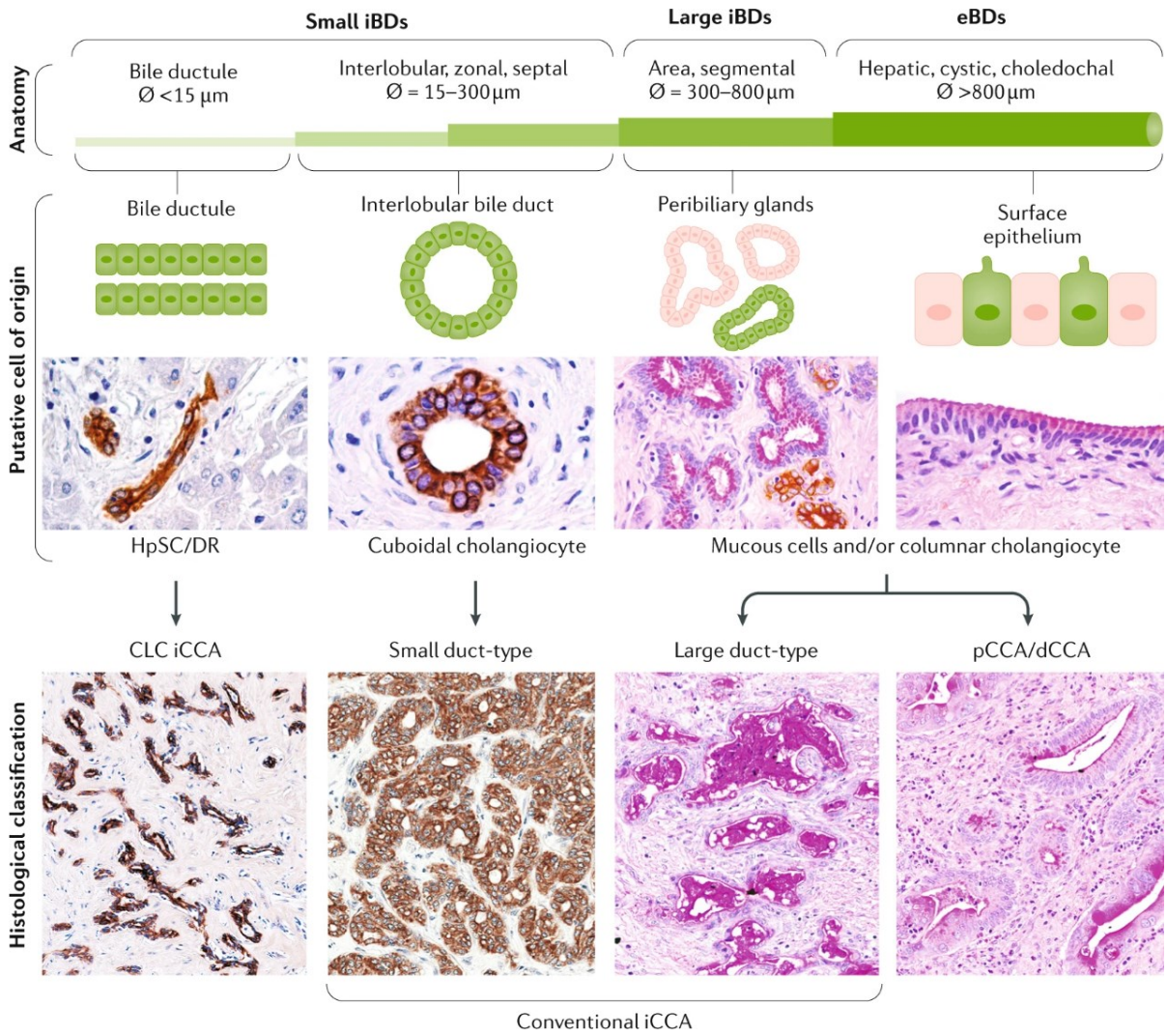

Figure 3. Histological subtypes in CCA and putative cells of origin.
The intrahepatic biliary tree is divided into small and large bile ducts (iBDs) based on duct size. Small iBDs are lined with cuboidal cholangiocytes, while large iBDs are lined with columnar, mucous cholangiocytes and contain peribiliary glands. The extrahepatic biliary tree (eBDs) resembles large iBDs anatomically. Histological subtypes of cholangiocarcinoma (CCA) reflect the characteristics of the affected ducts and their cells of origin. Small bile duct iCCA arises in small iBDs, likely originating from cuboidal cholangiocytes, whereas large bile duct iCCA involves large iBDs, with columnar cholangiocytes and peribiliary glands as the probable source. Cholangiolocarcinoma (CLC), a variant of iCCA, probably originates from human pluripotent stem cell (HpSC) or ductular reactions (DR) seen in chronic liver disease. Finally, pCCA and dCCA are thought to arise from the epithelial lining and peribiliary glands (adapted from Banales *et al*., 2020).

Interestingly, the histological classification reflects the significant molecular diversity of CCAs. This histological classification correlates with specific clinical, pathological, and molecular features. Emerging evidence have demonstrated that small bile duct iCCA type is often linked to specific mutations, including IDH1/IDH2 mutations and FGFR2 fusions, while the large bile duct iCCA, similar to pCCA and dCCA, is mainly

associated with KRAS and TP53 mutations. Additionally, dCCA often involves ELF3 mutations[1,2,6,12].

1.2 Signaling and molecular networks in cholangiocarcinoma etiopathogenesis

Cholangiocarcinogenesis is a multi-step process that involves interactions between pro-inflammatory cytokines, growth factors, bile acids, and other extracellular ligands within the tumor microenvironment[1,2] (Fig. 4). These factors stimulate abnormal activation of cell surface receptors and deregulate intracellular signaling, promoting cell proliferation, survival, and genetic or epigenetic changes. In addition, it has been demonstrated that CCA often develops in the context of chronic biliary inflammation or cholestasis, which drives carcinogenesis. In fact, inflammatory process is generally associated with activation of immune-related signaling pathways, while alterations in cell proliferation are mainly due to the activation of oncogenic pathways, including receptor tyrosine kinase (RTK) signaling, RAS–RAF–ERK, PI3K–AKT–mTOR, and mutations in KRAS, along with stem-like genomic traits and Hippo pathway alterations such as *SAV1* deletion[1,2,13].

Regarding the role of inflammatory mediated signaling pathways, it has been demonstrated that chronic inflammation and fibrosis promote cholangiocyte transformation through the hyperactivation of IL-6–STAT3 signaling that supports cell proliferation by regulating MCL1 and modifying EGFR promoter methylation[14,15]. Similarly, bile acids contribute to cholangiocarcinogenesis by activating EGFR, inducing COX2, MCL1, and IL-6, and suppressing Farnesoid X Receptor (FXR), whose decreased expression correlates with tumor differentiation[16].

In iCCA and pCCA, several evidence have demonstrated that cancer-associated fibroblasts (CAFs) promote tumor growth through paracrine factors like Heparin-binding EGF-like Growth Factor (HB-EGF), Stromal-cell derived Factor 1 (SDF1), Platelet-derived Growth Factor (PDGF)-B and Extracellular Matrix (ECM)

proteins[17,18]. Despite the high variability, RTK signaling alterations is a common pathway in CCA[1,2,19]. In particular, KRAS mutations are widespread in all CCA subtypes, while BRAF mutations and FGFR2 or ROS1 fusions are more specific to iCCA[19–23]. In addition, IDH1 and IDH2 mutations produce the oncometabolite 2-hydroxyglutarate, which disrupts epigenetic regulation by inhibiting DNA and histone demethylases[24,25]. This event leads to mitochondrial dysfunction and epigenetic silencing, including reduced ARID1A expression due to hypermethylation. Mutations in chromatin-remodeling genes, such as BAP1, ARID1A, and PBRM1, are also frequent in iCCA, contributing to tumor development[26].

Moreover, several pathways involved in development such as Notch, WNT–β-catenin, and Hippo–YAP are markedly active in iCCA, particularly during liver repair and inflammation, which are key risk factors for iCCA[27]. In particular, the overexpression of Notch receptors contributes to both iCCA and eCCA subtypes by driving hepatocyte-to-cholangiocyte transdifferentiation during carcinogenesis[28]. Noteworthy, evidence have shown that SOX17 is hypermethylated in CCA tissues compared with healthy tissue. SOX17, a WNT pathway inhibitor, acts as a tumor suppressor by regulating cholangiocyte differentiation[29].

The Hippo-YAP signaling pathway controls cell proliferation and organ size. YAP, a transcriptional co-activator, is normally inhibited by Hippo proteins (MST1/MST2) but can become active through Hippo-independent mechanisms such as inflammation and ECM alterations. Several studies have reported increased YAP nuclear expression in CCA specimens and correlation with a poor prognosis[30,31]. *In vitro* studies have demonstrated that YAP is activated by IL-6, PDGF, and fibroblast growth factors, forming a feed-forward loop involving FGFR1, FGFR2, and FGFR4[32].

In conclusion, cholangiocarcinogenesis involves a multifaceted interaction between extracellular ligands, such as pro-inflammatory cytokines, growth factors, and bile acids, within the tumor microenvironment (TME). These ligands drive increased expression or abnormal activation of cell surface receptors, disrupting intracellular

signaling pathways and ultimately promoting cell proliferation, survival, and genetic or epigenetic changes[20,21,33].

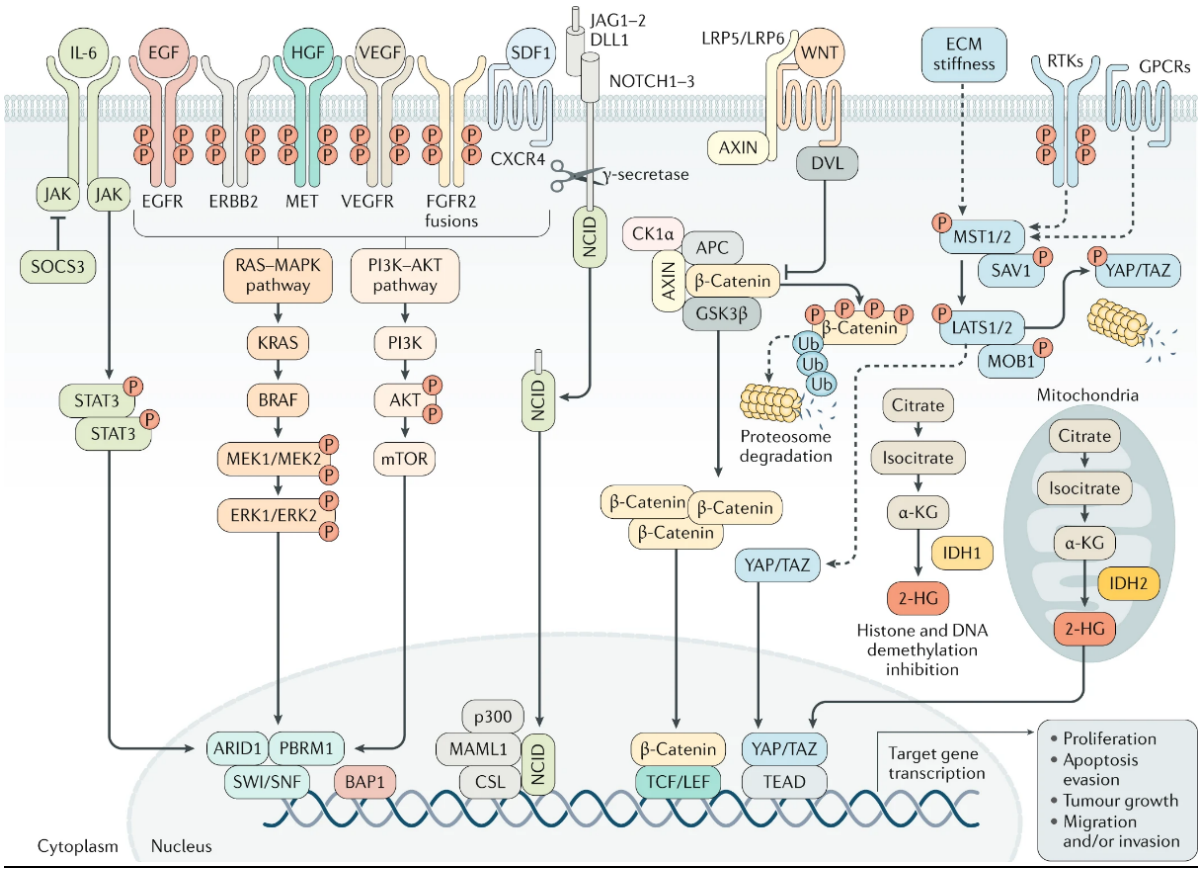

Figure 4. Intracellular pathways involved in CCA development and progression.
Schematic representation of signaling pathways involved in cell proliferation, survival, migration, and invasion in CCA. This scheme includes interactions between extracellular ligands, such as pro-inflammatory cytokines, growth factors, and bile acids, within the tumor microenvironment, coupled with increased expression or abnormal activation of cell surface receptors and deregulated intracellular signaling pathways (adapted from Banales *et al*., 2020)

1.3 Epidemiological trends and therapeutic approaches

Despite CCA is considered as a rare cancer, both the overall incidence and the global mortality rate have increased progressively worldwide over the past four decades, according to the World Health Organization and Pan American Health Organization databases for 32 selected locations in Europe, America, Asia and Oceania[1,34]. The three subtypes of CCA (iCCA, pCCA and dCCA) exhibit variations in risk factors and epidemiological patterns. While the overall rates of CCA in Asia have remained

unchanged, the incidence of iCCA has shown a consistent rise in most Western countries, whereas the rates of both dCCA and pCCA have either stabilized or declined. Interestingly, the highest rate globally has been reported in northeastern Thailand (85 per 100,000), whereas the lowest in Canada (0.4 per 100,000)[35].

According to the previously mentioned databases, mortality rates are higher in men compared to women and are generally more elevated in Asian countries compared to Western regions. Japan reports the highest mortality among men (2.81 per 100,000), while in the USA, the increase in mortality from 2004 to 2014 was most pronounced among African American individuals (45%), followed by Asian (22%) and non-Hispanic whites (20%) individuals[36,37].

In regions where liver fluke infection is common (e.g. Indochina, China and Korea), the of this form of cancer incidence is up to 40 times higher compared to Europe, USA and Australasia (0.3-3.5 cases per 100 000 population)[37].

Furthermore, the chronic inflammation of the biliary epithelium, such as primary sclerosing cholangitis (PSC), or other pathological conditions like hepatolithiasis, are recognized as characteristic risk factors for CCA development. Patients with PSC in Western countries and those with hepatobiliary flukes or hepatolithiasis in Asian countries show an increased probability to develop CCA. Other recognized risk factors contributing to increasing CCA rates are high alcohol consumption, tobacco smoking and viral infections (hepatitis B virus (HBV) and hepatitis C virus (HCV))[38,39].

Based on combined incidence and mortality data, CCA is clearly a significant global public health concern. Furthermore, CCA is often diagnosed at advanced stages due to nonspecific symptoms. Indeed, approximately 70% of CCA patients have inoperable disease at the time of diagnosis, limiting treatment options to supportive care[1,2,40].

According to current guidelines regarding clinical management of patients diagnosed with CCA, the treatment strategy varies for each type of cancer depending on its stage. The treatment algorithm, shown in Fig. 5, reports current gold standard treatment for biliary tract cancer (BTC), including both CCA and gallbladder carcinoma (GBC), a rare aggressive tumor arising from the gallbladder or cystic duct[40].

Only approximately 25–30% of patients with CCA are diagnosed with early-stage disease and qualify for curative surgery. Unfortunately, CCA is associated with a high post-surgical relapse rate (up to 80%), which has led to the consideration of adjuvant chemotherapy as a therapeutic strategy[1,7,41]. A number of clinical studies have been reported, in which all patients with resected BTC were randomly assigned to observation alone or chemotherapy. Among all the phase III randomized clinical studies performed, the BILCAP study marked a significant milestone in the treatment of CCA. This randomized, controlled, multicenter phase III trial was conducted across 44 specialist hepatopancreatobiliary centers in the UK. Patients were randomly assigned in a 1:1 ratio to receive either oral capecitabine or observation. The study showed a partial benefit from adjuvant capecitabine when compared with observation alone, both in terms of overall survival (OS, HR 0.71) and relapse-free survival (RFS, HR 0.75)[1,41]. Based on BILCAP results, since 2019 international guidelines have recommended adjuvant capecitabine for six months following surgical resection as the standard of care[42].

CCA patients with locally advanced or metastatic disease are not suitable for surgery. In localized and/or metastatic unresectable disease, treatment with a chemotherapeutic combination of Cisplatin and Gembcitabine, followed by immunotherapy with Durvalumab, a monoclonal antibody against Programmed death-ligand 1 (PD-L1) is the only therapeutic strategy available[1,2].

Progression after first-line therapy is unfortunately very common in patients with CCA. In cases of progression, mutational profiling analyses have demonstrated that nearly 40% of patients exhibit genetic alterations that could serve as potential targets for precision medicine[19,21,24]. Based on these findings, international guidelines now include targeted therapies as viable treatment options (e.g., inhibitors of IDH1 (Ivosidenib), FGFR2 fusion (Pemigatinib, Infigratinib, Futibatinib), and BRAF (Dabrafenib, Trametinib), anti-HER2 agents (Trastuzumab, Pertuzumab), or immunotherapy (Pembrolizumab) for cases with microsatellite instability and/or mismatch repair deficiency)[5,23,41].

Finally, 5-fluorouracil–leucovorin–oxaliplatin (FOLFOX) or 5-Fluorouracil (5-FU) combined with nano-liposomal irinotecan (nal-iri) can be used as second line setting after failure of first-line cisplatin–gemcitabine and/or in patients not suitable for targeted approaches[1].

Despite considerable efforts by the scientific community to improve the management of these patients, the prognosis remains poor, with no significant improvements observed in quality of life.

Furthermore, numerous studies have demonstrated that cholangiocarcinoma is a highly chemoresistant tumor[2,18]. Several resistance mechanisms have been identified, including alterations in genes regulating drug uptake, export, and metabolism, changes at the target level, mutations affecting DNA repair mechanisms, and modifications of key factors involved in apoptosis and cell survival[2].

These findings underscore the critical need for deeper insights into tumor biology, particularly non-genetic molecular mechanisms, to uncover new biomarkers for predicting prognosis and treatment response, as well as to identify innovative therapeutic targets.

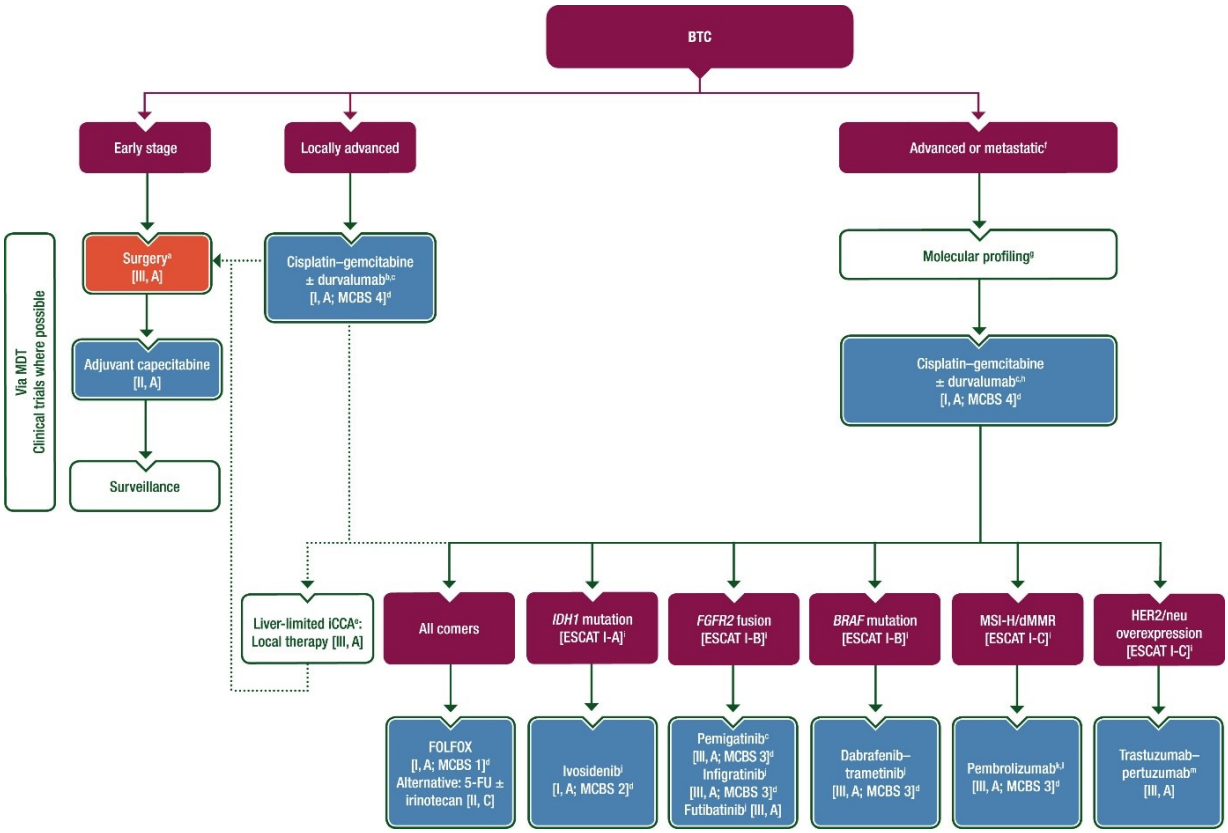

Figure 5. Flow chart representing clinical management of CCA patients.

Schematic representation of current therapeutic approaches for CCA patients according to current formal guidelines. Purple: general categories or stratification; red: surgery; white: other aspects of management; blue: systemic anticancer therapy (adapted from Vogel *et al*., 2023).

2. Primary cilia in human diseases and cancer

2.1 Cilia: structure and function

Cilia are evolutionarily conserved, microtubule-based cellular organelles that protrude from the surface of many epithelial cells. These extracellular structures are broadly classified into two main functional groups: motile cilia and non-motile cilia, also known as primary cilia. Motile and non-motile cilia differ in distribution, function, and structure[43,44].

Motile cilia are typically present in clusters, with more than 100 copies per cell, projecting from the surface of epithelial cells in specialized tissues. Their functions vary depending on the organ and cell type, often involving coordinated beating to move

liquids or mucus across tissue surfaces[44]. For example, multiciliated cells in the spinal cord and brain ventricles of adults help drive cerebrospinal fluid flow and guide the directional migration of neuroblasts[45]. Similarly, epithelial cells in the respiratory system use cilia to facilitate mucociliary clearance[46], while those in the fallopian tubes propel oocytes toward the uterus[47]. Additionally, motile cilia play a crucial role in embryonic development by establishing left-right axis determination in the embryonic node[48].

In contrast, primary cilia are single, non-motile sensory organelles present on the surface of most epithelial cells[43,44]. Several evidence have suggested that these non-motile cilia function as transduction hubs, receiving and transmitting extracellular signals into the cell. This signaling regulates various cellular processes, including growth, differentiation, and development[49].

Structurally, both motile and non-motile cilia share a dynamic composition comprising two main subunits: the basal body and the axoneme[43,50,51] (Fig. 6). The basal body is a barrel-shaped microtubular structure located near the cell surface, forming the base of the cilium and originating from the centrosome. The centrosome itself is a cytoplasmic organelle consisting of two centrioles, known as the mother and daughter centrioles, along with associated centriole satellites.

The axoneme is a cytoskeletal extension anchored to the basal body that protrudes out of the cell[50]. The primary structural distinction between the two types of cilia lies in the axoneme. In motile cilia, the axoneme consists of nine microtubule doublets arranged around a central pair, with dynein arms enabling motility—commonly referred to as the "9+2" pattern. In contrast, primary cilia lack the central pair and dynein arms, resulting in a non-motile "9+0" pattern[50,51].

Exceptions to this dichotomous classification include motile cilia in the embryonic node, which exhibit a “9+0” pattern, and “9+2” non-motile cilia found in the auditory and olfactory systems[44].

Finally, an important ciliary structure is the transition zone, a specialized domain located between the basal body and axoneme, functioning as a gate that regulates the import and export of various molecular cargos within the cilium[43,50].

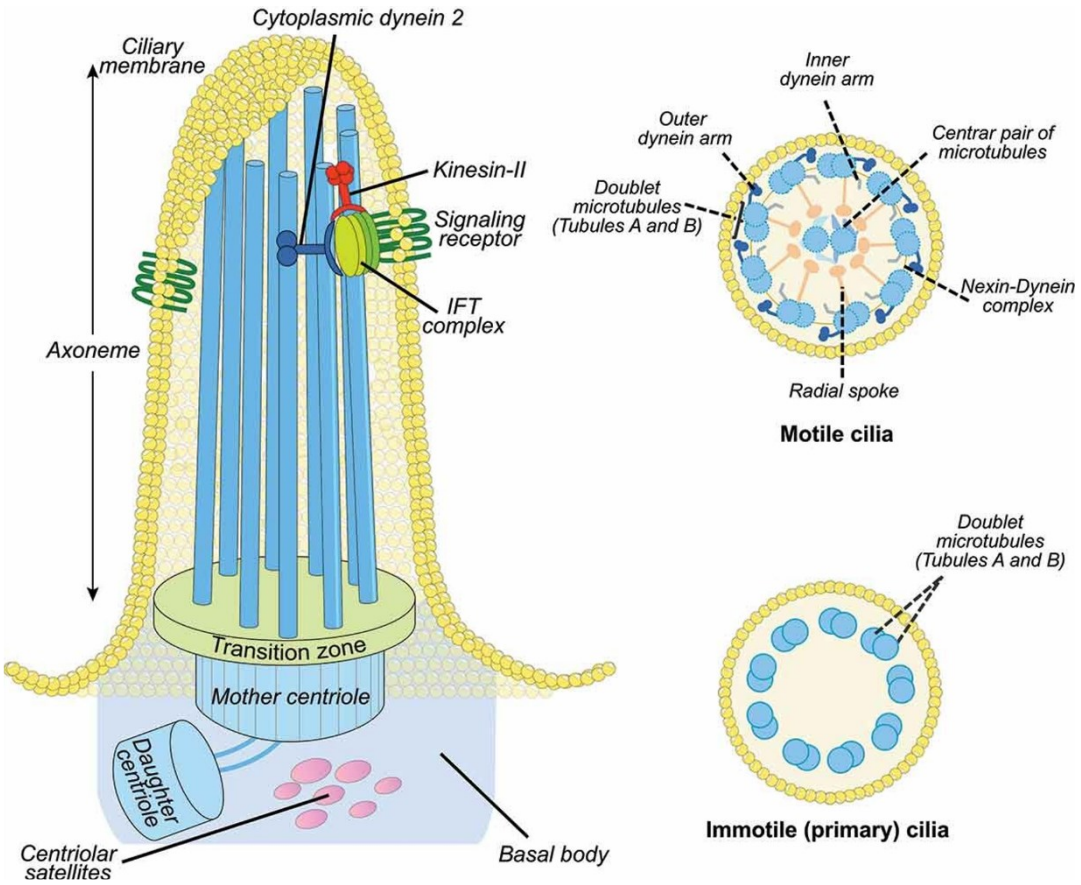

Figure 6. Schematic representation of cilia structure.
Left: scheme of structural components in cilia. The axoneme, originating from the basal body (mother centriole), consists of nine microtubule doublets extending from the ciliary membrane. Intraflagellar transport (IFT) within the axoneme is powered by kinesin-II motors (toward the tip) and cytoplasmic dynein 2 motors (toward the base). The transition zone, located at the axoneme base, regulates interactions with the ciliary membrane. Right: motile cilia feature a "9+2" arrangement with a central microtubule pair, radial spokes, and dynein arms, enabling movement. In contrast, immotile primary cilia have a "9+0" configuration, lacking both the central pair and dynein arms (adapted from Morleo *et al*., 2023).

2.2 Congenital disorders affecting cilia: the ciliopathies

Over the years, biomedical interest in cilia has been fueled by the discovery of an increasing number of inherited disorders, known as ciliopathies, which arise from mutations in genes encoding proteins involved in cilia assembly, function, or localization within various ciliary structures[52,53]. Ciliopathies comprise a wide range of

severe genetic disorders characterized by a spectrum of phenotypes affecting multiple organs, such as central nervous system, eyes, skeleton and visceral organs, like kidneys and liver[54] (Fig. 7).

Ciliopathies can arise from defects in ciliary proteins responsible for the assembly and function of motile cilia, giving rise to so called motile ciliopathies, or from disruptions in proteins critical to the assembly and function of immotile cilia, thus causing sensory ciliopathies. Additionally, non-ciliary proteins can influence ciliary functions and contribute to ciliopathies[53].

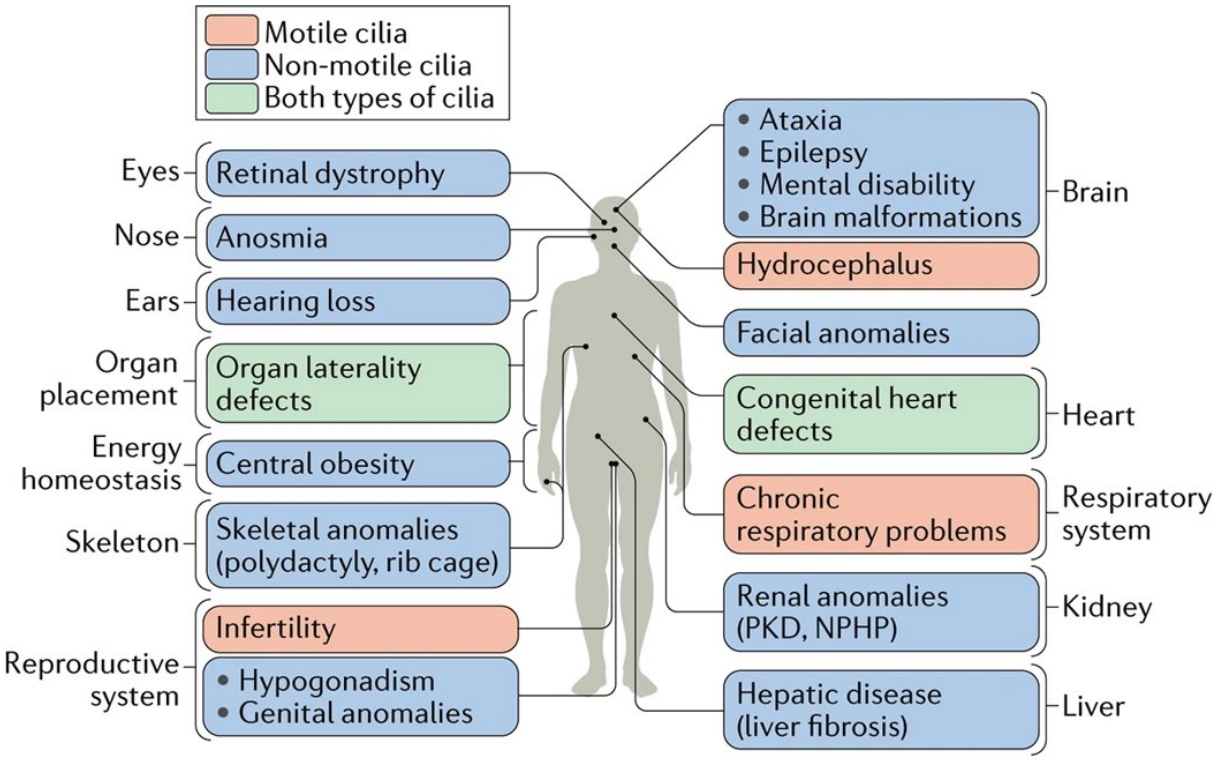

Figure 7. Ciliopathies affect multiple human organ systems.

The figure illustrates the various organ systems and tissues impacted by different ciliopathies, highlighting the primary phenotypic manifestations in each organ. Ciliopathies arising primarily from defects in motile cilia are marked in orange, those caused by non-motile (primary) cilia defects are indicated in blue, and those associated with abnormalities in both types of cilia are shown in green. Abbreviations: NPHP nephronophthisis, PKD polycystic kidney disease (adapted from Reiter J. *et al*., 2017).

Motile ciliopathies result from defects in the formation or function of motile cilia, impairing movement and fluid flow. These dysfunctions compromise mucus clearance, leading to chronic airway diseases, and can also affect establishment of laterality,

fertility, and brain development. The most prevalent motile ciliopathy is Primary Ciliary Dyskinesia (PCD, OMIM: #244400)[52–55].

Conversely, sensory ciliopathies arise from defects in the sensory or signaling functions of non-motile primary cilia. Examples include Bardet-Biedl Syndrome (BBS, OMIM #209900), a multisystem disorder characterized by developmental abnormalities and degenerative features; Leber Congenital Amaurosis (LCA, OMIM #204000), which results in early-onset vision loss; and Oral-Facial-Digital Type 1 Syndrome (OFDI, OMIM #311200), an X-linked disorder that leads to oral, facial, and digital malformations, as well as renal and central nervous system (CNS) abnormalities in females[52,53].

Other ciliopathies include Autosomal Dominant Polycystic Kidney Disease (ADPKD, OMIM: #173900) and Autosomal Recessive Polycystic Kidney Disease (ARPKD, OMIM: #263200), both of which are characterized by the progressive formation of kidney cysts that ultimately lead to renal failure. Additional examples include Joubert Syndrome (JBTS, OMIM: #213300), which is marked by distinctive cerebellar and brainstem malformations, along with associated features such as hypotonia, ataxia, psychomotor delay, irregular breathing patterns, and oculomotor apraxia. Nephronophthisis (NPHP, OMIM: #256100) and Meckel-Gruber Syndrome (MKS, OMIM: #249000) also fall under this category, with phenotypic manifestations that include brain abnormalities, skeletal dysplasia, and cyst formation in kidney and liver[52].

Finally, it is well established that while many syndromic ciliopathies—such as OFDI, BBS, JBTS, NPHP, and MKS—are rare, conditions like ADPKD are relatively more common[55].

2.3 Primary cilia in cancer

Ciliogenesis is a tightly regulated process occurring at multiple levels. The primary cilium is a highly dynamic organelle, not only because it is assembled during specific phases of the cell cycle but also due to the active molecular transport within its axoneme[56]. During ciliogenesis, cilia elongate from the basal body through the addition of new axonemal subunits, organized into macromolecular particles, at the distal tip. Furthermore, primary cilia formation is strictly dependent on the cell cycle phase. The primary cilium forms during the post-mitotic G0/G1 phase and disassembles at the G2/M transition. After cell division is complete, the cilium reassembles in the subsequent G1 phase[57]. Thus, growth-arrested cells are predominantly ciliated, whereas re-entry into the cell cycle, triggered by growth factor or hormone stimulation, induces cilium resorption. Additional conditions that promote cilia biogenesis include starvation and cell confluency, both of which drive the cell into a non-mitotic state[56]. Moreover, cilia function as complex sensory organelles, participating in the signal transduction of several cancer-related pathways and contributing to cell cycle regulation[54,58] (Fig. 8). Examples of signaling pathways transducing by cilia: Hedgehog (Hh), Notch, Wingless-related integration site (Wnt), Hippo, Platelet-derived Growth Factor Receptor α (PDGFRα), Epidermal Growth Factor Receptor (EGFR), Transforming Growth Factor-β (TGF-β), Fibroblast Growth Factor Receptor (FGFR), Polycystin-1 and Polycystin-2 (PKD1/2), DNA Damage Response (DDR) and the mammalian target of rapamycin (mTOR). Primary cilia play a pivotal role in regulating numerous cellular processes, including tissue homeostasis, cell fate determination, proliferation, survival, and migration[49,58].

Several evidence have demonstrated that alterations in cilia structure and/or function are clearly linked to uncontrolled cell proliferation and oncogenesis[56,58]. However, the role of the primary cilium in cancer remains a topic of debate. Some studies indicate that in medulloblastoma and basal cell carcinoma, smoothened-dependent tumors rely on the presence of primary cilia for their development. Conversely, in most solid

malignancies—such as pancreatic, breast, melanoma, cholangiocarcinoma, glioblastoma, prostate, and ovarian cancers—primary cilia are diminished or entirely absent in tumor cells[58]. This loss suggests that the absence of cilia is a frequent occurrence in neoplastic transformation, supporting the idea that the primary cilium functions as a potential tumor suppressor organelle[59,60].

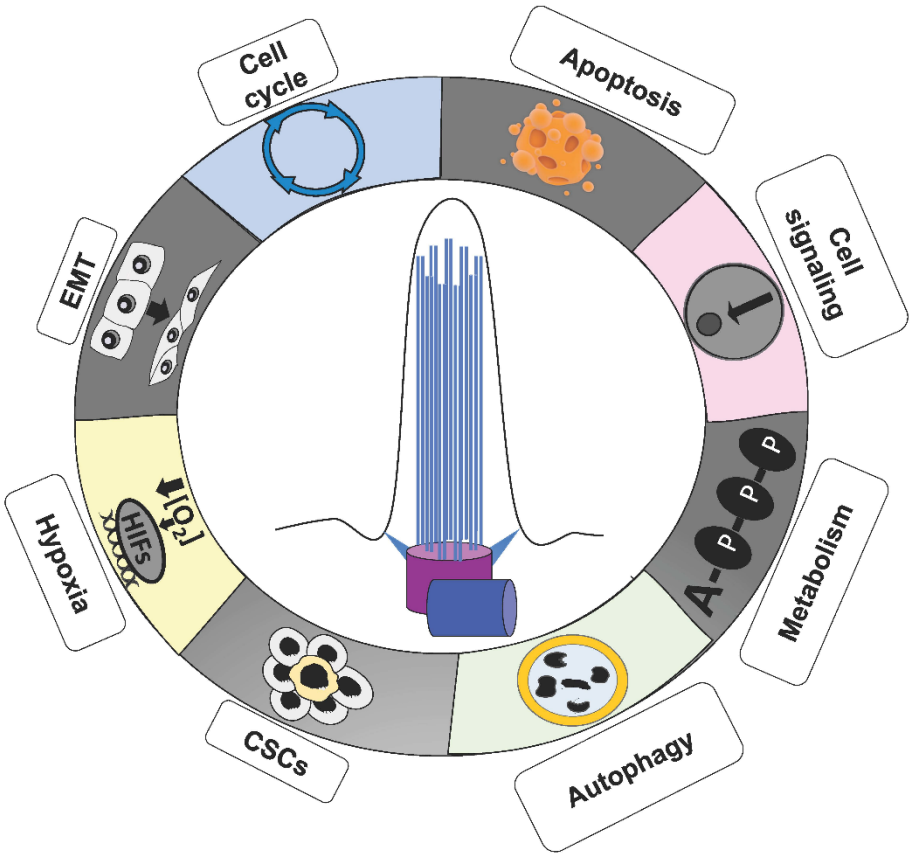

Figure 8. Signaling pathways coordinated by primary cilia.
The primary cilium is a sensory organelle that functions as an antenna, capturing external signals and transmitting them into the cell to engage various cellular pathways. Abbreviations: CSCs, cancer stem cells, EMT epithelial-to-mesenchymal transition (adapted from Fabbri *et al*., 2019).

3. Ciliary genes as possible candidate therapeutic targets or biomarkers in cancer

The advent of next-generation sequencing (NGS) technologies and the implementation of multi-omics approaches have identified several ciliary genes altered in human cancers, suggesting the hypothesis that primary cilium may represent a pivotal player in cancer progression[49,60].

The functional interplay between primary cilia and the cell cycle is well established. In many highly proliferative cancer cells primary cilia are absent, suggesting that cilia loss may drive mitosis and, consequently, cell proliferation. Several protein kinases, including Polo-like Kinase 1 (PLK1), Aurora Kinase A (AURKA), NIMA related Kinase 2 (NEK2), and Kinesin Family member 24 (KIF24), are key regulators of mitotic events and play crucial roles in centrosome maturation. These kinases phosphorylate centrosomal proteins and are implicated in various oncogenic processes[58,60].

PLK1 is essential during the M phase of the cell cycle, as its kinase activity promotes primary cilia disassembly before mitotic entry. PLK1 is overexpressed in numerous human cancers and is thought to promote tumorigenesis[58,61]. AURKA, a centrosomal mitotic kinase, regulates S-phase entry and is activated by the scaffold protein Human Enhancer of Filamentation 1 (HEF1) in the presence of calcium. Once activated, AURKA triggers Histone deacetylase 6 (HDAC6), which destabilizes axonemal microtubules, leading to primary cilia disassembly[62]. AURKA has been found to be upregulated in non-ciliated ovarian and renal cell carcinoma cells. Interestingly, HDAC6 inhibition has been shown to restore PCs in chondrosarcoma and cholangiocarcinoma cells, suppressing cell proliferation and invasive capacity[59]. Similarly, HEF1 overexpression has been associated with increased cell migration and cancer progression in tumors such as breast cancer, melanoma and colorectal cancer[62,63].

NEK2 is another critical regulator of centrosome and basal body functions. It promotes axonemal microtubule disassembly by phosphorylating KIF24, a microtubule-based motor protein that stimulates microtubule-depolymerizing activity, thereby preventing cilia formation in proliferating cells. Both NEK2 and KIF24 are overexpressed in multiple cancers[60]. Notably, inhibiting these proteins in cilia-deficient breast cancer cell lines has been shown to restore ciliogenesis, reducing cancer growth[58,64].

Moreover, large-scale genomic studies have provided substantial evidence linking ciliary genes and structures to the regulation of various signaling pathways and

biological processes. For instance, Intraflagellar Transport proteins (IFTs) are associated with Notch signaling and autophagy. Specifically, Intraflagellar Transport protein 20 (IFT20) plays a critical role in the biogenesis and function of lysosomal autophagy by regulating the lysosomal targeting of acid hydrolases[65]. Several studies have demonstrated that the knockdown of IFTs disrupts Notch signaling and impairs progenitor cell differentiation during skin development[66]. Recently, the role for IFT20 repression in inhibiting breast cancer cell migration has also been described[67].

Furthermore, the genes associated with Bardet–Biedl syndrome (BBS1, BBS4, and MKKS), which encode basal body proteins, regulate components of the oncogenetic signaling pathway Wnt. In fact, suppression of these genes leads to the stabilization of β-catenin, resulting in hyperactivation of the Wnt signaling response in cultured cells[60]. Additionally, NPHP4, a ciliary protein mutated in nephronophthisis, has been identified as a potent negative regulator of the tumor-suppressive Hippo pathway[68]. Notably, several NPHP-related proteins have been found to be upregulated in various tumors, including breast, pancreatic, and colorectal cancers[60].

The Centrosomal Protein 164 (CEP164) has also been implicated in cancer biology. CEP164 interacts with the DNA Damage Response (DDR)-related protein ATM and undergoes phosphorylation in response to DNA damage. Its downregulation is associated with reduced phosphorylation of other DDR proteins, such as Checkpoint Kinases 1 and 2 (CHK1/2), highlighting its role in maintaining genomic integrity[69].

Furthermore, primary cilia regulate the mechanistic target of rapamycin (mTOR) pathway through the ciliary protein activation of Serine/Threonine Kinase 11 (STK11 or LKB1) LKB1. Depletion of LKB1 leads to the formation of pancreatic cystic tumors in mice, suggesting that the interplay between LKB1, the mTORC1 pathway, and primary cilia is a key factor in regulating tumorigenesis in pancreatic cancer[70].

Together, these findings underscore the significant but distinct roles of primary cilia across different cancer types, offering new avenues of research to further understand cancer biology and develop targeted therapies. This evidence strengthens the

hypothesis that *ciliotherapy* could represent a promising alternative approach for treating human cancers that remain challenging to address effectively.

4. The *OFD1* gene: linking ciliogenesis and cancer

4.1 The *OFD1* gene in human ciliopathies

The OFD1 gene was first identified on the X chromosome in 1983, as one of the earliest transcribed sequences mapped to the Xp22.2 locus. Initially referred to as CXORF5 (also known as 71-7A or DXS69E)[71], it was renamed OFD1 in 2001 following the discovery of mutations associated with oral-facial-digital syndrome type I, an X-linked dominant male-lethal developmental disorder linked to ciliary dysfunction[72].

The OFD1 protein serves as a paradigmatic example of a multitasking protein, performing diverse functions depending on cellular context, subcellular localization, and tissue type. It is predominantly localized to the centrosome, basal body, and pericentriolar satellites[73,74]. Both *in vitro* and *in vivo* studies have demonstrated its essential role in primary cilia formation and the establishment of left–right asymmetry[75]. Beyond its involvement in ciliogenesis, OFD1 also regulates protein content[76], restricts centriole length and distal structure[77], contributes to chromatin remodeling during DNA double-strand break repair[78], and facilitates cell cycle progression[79].

More recently, OFD1 was identified as a receptor involved in selective autophagy[51,80]. Notably, some of its pleiotropic roles, such as in autophagy, are independent of ciliogenesis. In addition to its primary localization, OFD1 has also been observed in the nucleus, where functions like chromatin remodeling may occur[81].

The gene OFD1 is primarily associated with oral-facial-digital syndrome type I (OFDI, OMIM #311200), an X-linked dominant disorder typically lethal in males. OFDI is characterized by dysmorphic facial features, malformations of the oral cavity, skeletal anomalies, and central nervous system (CNS) abnormalities. Affected females often

exhibit cystic kidney disease and, less frequently, cysts in the liver, pancreas, or ovaries. Common craniofacial features include facial asymmetry, hypertelorism, frontal bossing, and nasal and malar hypoplasia. Oral anomalies, such as cleft palate, hyperplastic oral frenula, and abnormal dentition, are prevalent, along with skeletal defects like syndactyly, brachydactyly, and polydactyly. Approximately 50% of patients present CNS anomalies, such as agenesis of the corpus callosum or cognitive impairment, and hearing defects are occasionally reported. While OFD1 mutations, often frameshift, missense, nonsense, or splicing alterations, are the genetic basis of OFDI, the disorder exhibits significant clinical variability, influenced by factors such as X-inactivation patterns[52,55,82].

Additionally, genetic alterations of OFD1 have been linked to four X-linked recessive disorders: Joubert syndrome 10 (JBS10, OMIM #300804), retinitis pigmentosa 23 (RP23, OMIM #300424), primary ciliary dyskinesia (PCD, OMIM #244400), and Simpson–Golabi–Behmel syndrome type 2 (SGBS2, OMIM #300209)[82,83] (Fig. 9).

In 2006, OFD1 was initially identified as the gene responsible for a novel syndrome characterized by intellectual disabilities, macrocephaly, obesity, skeletal anomalies, and ciliary dysfunction, termed SGBS2. However, later studies revealed that mutations in the Phosphatidylinositol Glycan Anchor Biosynthesis Class A (*PIGA*) gene are responsible for the disease's pathogenesis. The *PIGA* gene encodes for the catalytic subunit of the glycosylphosphatidylinositol-N-acetylglucosaminyltransferase (GPI-GnT) complex that is involved in Glycosylphosphatidylinositol (GPI) anchor biosynthesis. Although subsequent reports have suggested that SGBS2 is associated with mutations in *PIGA* rather than alterations in *OFD1*, the original family described by Budny et al. presented a different scenario. In this family, all nine affected males, except for the index case, died in infancy due to respiratory problems caused by the introduction of a premature stop codon in the open reading frame of OFD1. Functional evaluation of their respiratory cilia revealed a lack of coordination and a significant reduction in beat frequency, ultimately leading to a diagnosis of PCD in this family.

This study provided the first evidence that OFD1 plays a critical role in regulating the function of motile cilia.[84].

In 2009, OFD1 mutations were implicated in JBS10, a ciliopathy marked by neurodevelopmental defects and the characteristic “molar tooth sign” brain malformation. JBS10 is also associated with retinal, renal, and liver involvement, as well as polydactyly and left-right asymmetry in affected males. Most cases are severe, with many pregnancies terminated due to significant malformations[85].

Furthermore, OFD1 mutations have been linked to RP23, where affected individuals exhibit progressive vision loss without extraocular symptoms[86]. Recently, OFD1 mutations were also associated with PCD, a motile ciliopathy affecting respiratory and reproductive tissues. Seven mutations, primarily in the C-terminal region, have been identified in patients with recurrent bronchitis, bronchiectasis, sinusitis, and otitis media. Structural ciliary abnormalities and impaired motility were observed in some cases[87,88]. These findings underscore the diverse phenotypic spectrum associated with OFD1 mutations across multiple ciliary dysfunction disorders.

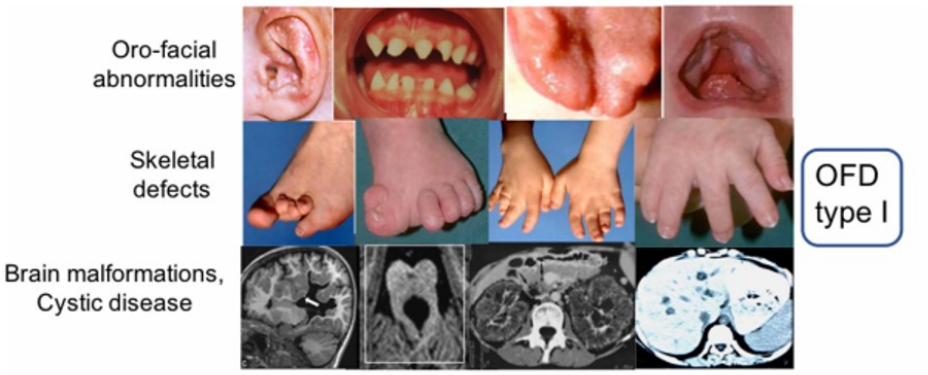

Oro facial defects (see above). Cystic disease affecting kidneys, liver, pancreas and/or ovaries. Skeletal defects. Brain abnormalities (intracerebral cysts, agenesis of the corpus callosum, and cerebellar agenesis).	Oro-facio-digital syndrome type 1 (OFD1; OMIM #311200)
Facial dysmorphisms. Developmental delay, brain abnormalities (molar tooth sign), retinal degeneration, digit abnormalities (polydactyly).	Joubert syndrome 10 (JS 10; OMIM #300804)
Macrocephaly, facial dysmorphisms, intellectual disability, ciliary dyskinesia, obesity, digit abnormalities.	Simpson-Golabi-Behmel syndrome type 2 (SGBS2; OMIM # 300209)
Early onset retinitis pigmentosa.	Retinitis Pigmentosa 23 (RP23; OMIM# 300424)
Neonatal respiratory distress, recurrent sinusitis and bronchitis. Bronchiectasis. Increased weight. Cilia disfunction. Skeletal defects. Occasional mild mental developmental delay and intellectual disability.	Primary ciliary dyskinesia (PCD)

Figure 9. Clinical features associated with OFD1 mutations.

The upper section highlights the most common phenotypes seen in OFD type I patients. Top row: orofacial abnormalities, including (from left to right) facial milia, dental anomalies with aberrant frenula, tongue malformations, and cleft palate. Middle row: skeletal defects affecting the upper and lower limbs, such as clinodactyly, brachydactyly, syndactyly, and, less frequently, polydactyly. Bottom row: brain malformations and renal cystic disease, including (from left to right) polymicrogyria (arrow), a rare instance of the molar tooth sign in a female with OFD type I, and cystic involvement of the kidneys and liver. The lower section illustrates clinical features associated with other conditions caused by OFD1 transcript mutations (adapted from Morleo *et al*., 2020).

4.2 The role of OFD1 in cancer

In recent decades, the OFD1 protein has emerged as a potential player in human cancer. While it is well-established that mutations in the OFD1 gene lead to ciliopathies, its role in cancer remains poorly understood, with only preliminary evidence available so far. The first indication of the possible involvement of OFD1 in cancer came from a study investigating the relationship between autophagy and primary cilia biogenesis[74]. The authors demonstrated, for the first time, that OFD1 at centriolar satellites plays a crucial role in suppressing primary ciliogenesis, whereas the fraction of OFD1 localized at centrioles is essential for cilia formation. Interestingly, in human breast cancer MCF7 cells, which typically do not form cilia, the forced downregulation of OFD1 at centriolar satellites induced the expression of cilia on the cell surface. Tang et al. first proposed OFD1 as a potential regulator of ciliogenesis in cancer [74].

Subsequent studies have investigated the role of OFD1 in other types of cancer. In oropharyngeal squamous cell carcinoma (OPSCC), it was observed that OFD1 expression is significantly elevated in HPV-positive patients, accompanied by a notable disruption of primary ciliogenesis[89].

More recently, a study of Kojima et al. reported abnormal accumulation of OFD1 in endometrial cancer (Fig. 10). The authors demonstrated a progressive increase in OFD1 levels in advanced stages of the disease. The increase in expression correlated with a significant reduction in the number of ciliated cells, suggesting a link between excessive proliferation and impaired ciliogenesis driven by aberrant OFD1 expression. The authors proposed that impaired autophagy, mediated by alterations in the levels of the autophagy receptor Sequestosome 1 (SQSTM1/p62), may underlie the increased OFD1 expression[90].

In conclusion, these findings demonstrate that OFD1 can influence ciliogenesis and cell growth, contributing to cancer development. This highlights the potential of OFD1 as a biomarker for cancer.

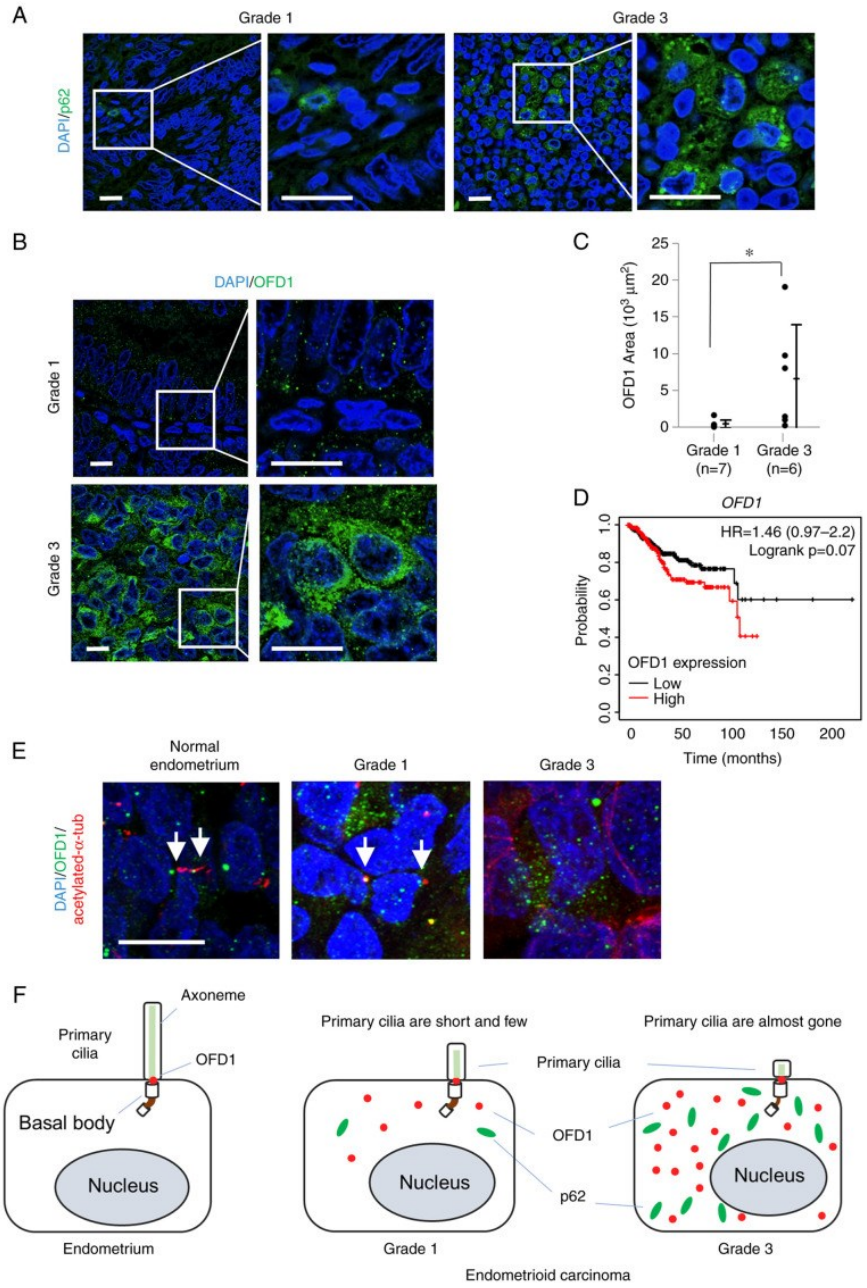

Figure 10. Relationship between primary cilia dysfunction and autophagy in endometrioid carcinoma.

Immunofluorescence staining on endometrial cancer samples reveals progressive accumulation of p62 (**A**) and OFD1 (**B**) as the disease advances from Grade 1 to Grade 3. The increase in OFD1 staining is quantified and validated using a dot plot of OFD1 intensity (**C**). Elevated OFD1 mRNA levels are associated with poorer patient survival, as shown in the Kaplan-Meier survival analysis (**D**). Fluorescence immunostaining for OFD1 and acetylated-α-tubulin highlights abnormal OFD1 overexpression in Grade 1 samples, with even greater accumulation in Grade 3, where a marked reduction in primary cilia is observed (**E**). A working model illustrates the relationship between primary cilia and autophagy in normal endometrial stromal cells compared to cells from endometrioid carcinoma Grades 1 and 3 (**F**) (adapted from Kojima *et al*., 2022).

Results

1. Identification of differentially expressed ciliary genes in cholangiocarcinoma

In order to identify genetic alterations of ciliary genes supporting cancerogenesis, we analyzed the expression profiles of primary cilium-associated genes using an RNA sequencing (RNA-Seq) approach. Specifically, total RNA was isolated from formalin-fixed, paraffin-embedded (FFPE) tissues obtained from a clinically annotated cohort of 80 CCA patients (Fig. 11). The cohort of CCA patients was collected in collaboration with Prof. Dominici at the Azienda Ospedaliera Universitaria of Modena, Italy.

Characteristic	N (%)
Age, years (median, range)	66 (36-88)
Gender	
Female	40 (57%)
Male	30 (43%)
ECOG PS	
0-1	54 (77%)
≥2	16 (23%)
Subsite	
iCCA	36 (51%)
eCCA	34 (49%)
Stage	
I-II	49 (70%)
III-IV	21 (30%)
Grading	
G1-G2	34 (48%)
G3-G4	36 (52%)
Angioinvasion	
Yes	40 (57%)
No	30 (43%)
Adjuvant chemotherapy	
Yes	41 (58%)
No	29 (42%)

Figure 11. Baseline demographic and clinicopathologic characteristics of the CCA cohort of patients.
The table summarizes the main features of the CCA cohort of patients analyzed (n= 80).

Tumor (T), stroma (ST) and normal (N) areas were identified by two pathologists after hematoxylin-eosin staining. RNAs from the areas of interest were isolated from FFPE macro or microdissected tissues using automated RNA extraction. A differential gene expression (DEG) analysis identified 6,315 DEGs when comparing T and ST areas and 3,392 between T and N areas, respectively (false discovery rate (FDR) <0.05). Among the DEG we identified a list of ciliary-related genes using a comprehensive database of ciliary genes, known as the Cilia Carta Database (Fig. 12A, B). Using a transcriptome analysis of CCA cohort, we thus obtained a signature of ciliary-associated genes.

Bioinformatic analysis identified OFD1 as the top-ranked cilium-associated gene. Notably, OFD1 was one of the most upregulated cilium-associated genes in tumor areas (fold-change ≥ 2.5, $p < 0.01$) (Fig. 12C). This observation led us to hypothesize that OFD1 might function as an oncogene in CCA.

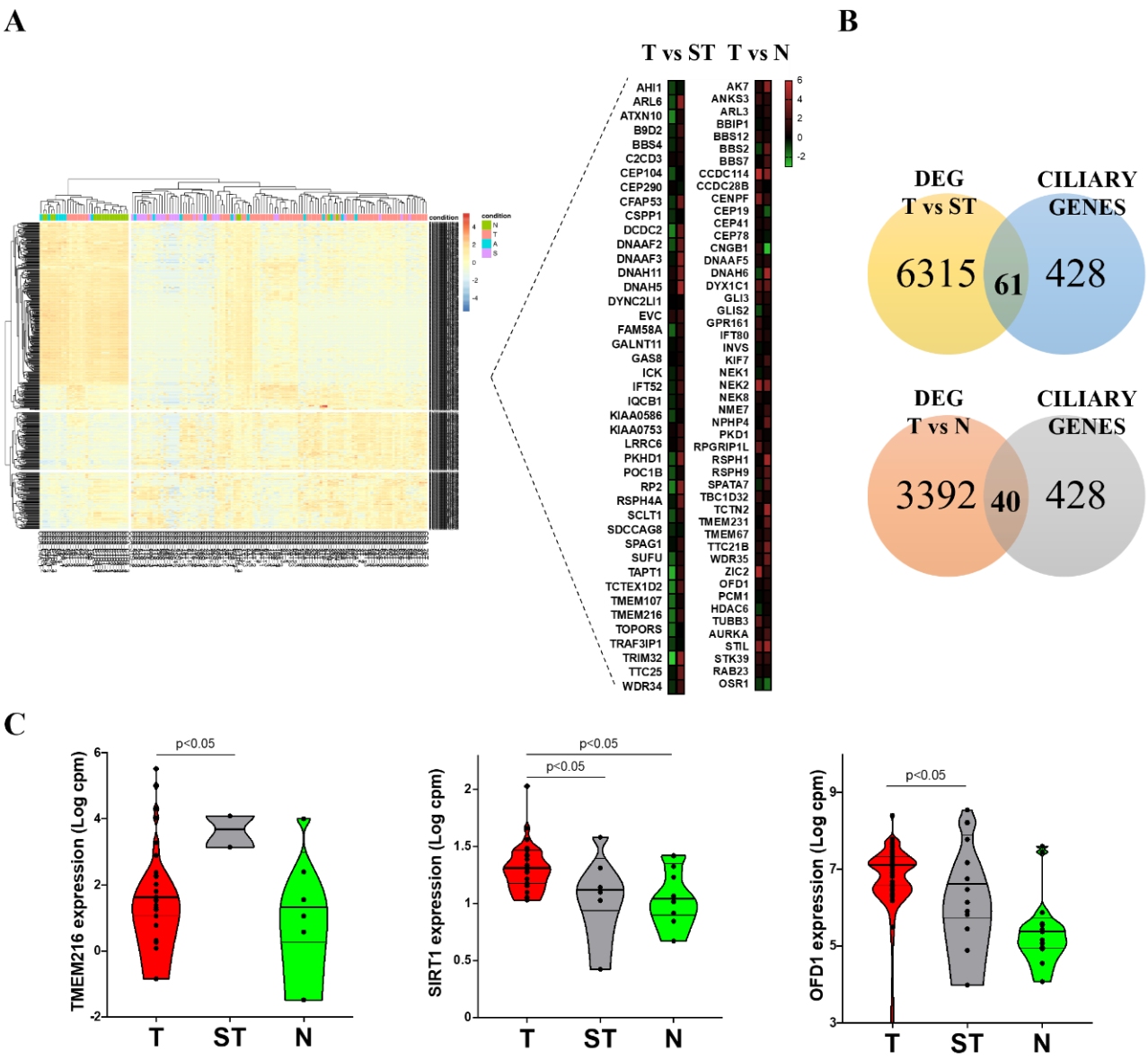

Figure 12. The transcriptomic profile of *Ciliome* in CCA patients.

Expression profile of cilium-associated genes in CCA patients. Heatmap demonstrating log relative expression level of differentially expressed genes (DEGs) between tumor and stroma (T vs ST) and tumor and normal (T vs N) areas of each patient. Cell colors (blue-white-orange-red gradient) correspond to the binary logarithm of the ratio of the expression level in a current sample to the average level across all the samples (per each gene) (**A**). Diagram showing the DE Ciliary Genes Analysis (**B**). Representative cilium-associated genes identified as the top-ranked dysregulated (fold-change ≥ 2.5, $p < 0.01$). Here, TMEM216, SIRT1 and OFD1 were shown (**C**).

2. Functional study of OFD1 in healthy human cholangiocytes and cholangiocarcinoma cell lines

2.1 OFD1 overexpression in healthy human cholangiocytes causes cilia reabsorption

Given the existing literature identifying OFD1 as a fundamental gene for ciliogenesis, we sought to assess the impact of OFD1 in healthy human cholangiocytes. To this end, we utilized the H69 human epithelial cholangiocyte cell line to generate OFD1-overexpressing cells. Using a lentiviral vector carrying the OFD1 gene under the control of a strong promoter (PLVX-cDNA hOFD1 vector), we successfully established OFD1-overexpressing H69 cells (H69 OE OFD1) to be used in *in vitro* experiments. As shown in Fig. 13, Real-Time PCR (RT-PCR) and Western blot analysis performed on H69 OE OFD1 cells revealed significantly higher OFD1 expression in the engineered cells compared to control cells in several cellular clones. We selected the H69 OE OFD1 #6 clone for our experiments due to the significant highest expression of OFD1 compared to H69 wild-type, as shown in both RT- PCR and Western blot analysis.

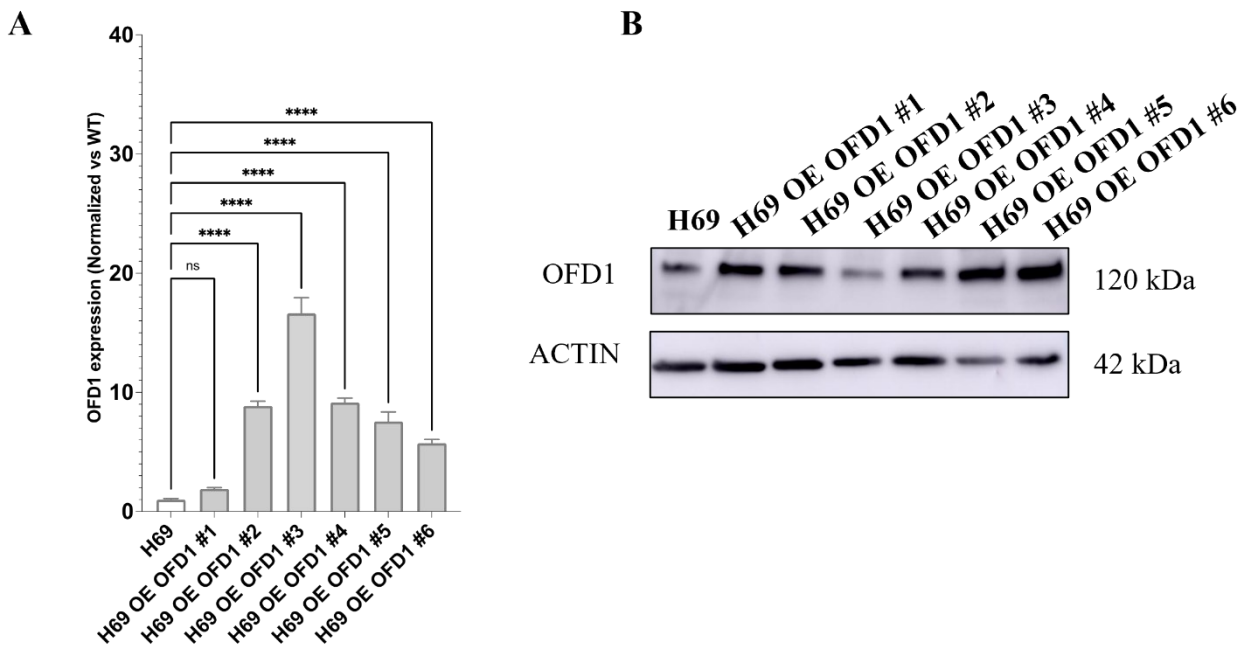

Figure 13. Generation of OFD1-overexpressing H69 clones.

OFD1 mRNA expression analysis using RT-PCR in H69 cells infected with OFD1-overexpressing lentiviral vector (H69 OE OFD1). H69 wild-type was used as relative control (**A**). Western blot analysis for OFD1 of protein lysates obtained from H69 wild-type and H69 OE OFD1. ACTIN was used as loading control (**B**). ****$p < 0.00001$; ns, not significative.

We further examined the effect of forced OFD1 overexpression on primary cilia formation in H69 cells by using immunofluorescence (IF) assays. IF experiments were performed by using H69 OE OFD1 cells following serum starvation as this condition promotes ciliogenesis. H69 wild-type cells were used as control. Cells were stained by using specific antibodies against OFD1 and ARL13B, as an axonemal marker (Fig. 14A). The results revealed that OFD1 overexpression significantly reduced ciliogenesis and markedly shortened cilia length compared to control cells. In fact, the number of ciliated cells, positive for ARL13B staining, was reduced from 38% to 3% comparing H69 to H69 OE OFD1 cells (Fig. 14B). In line with this evidence, the cilia length was reduced from 5,609 μm to 2,986 μm, thus supporting the hypothesis that OFD1 overexpression affected primary cilia biogenesis (Fig. 14C).

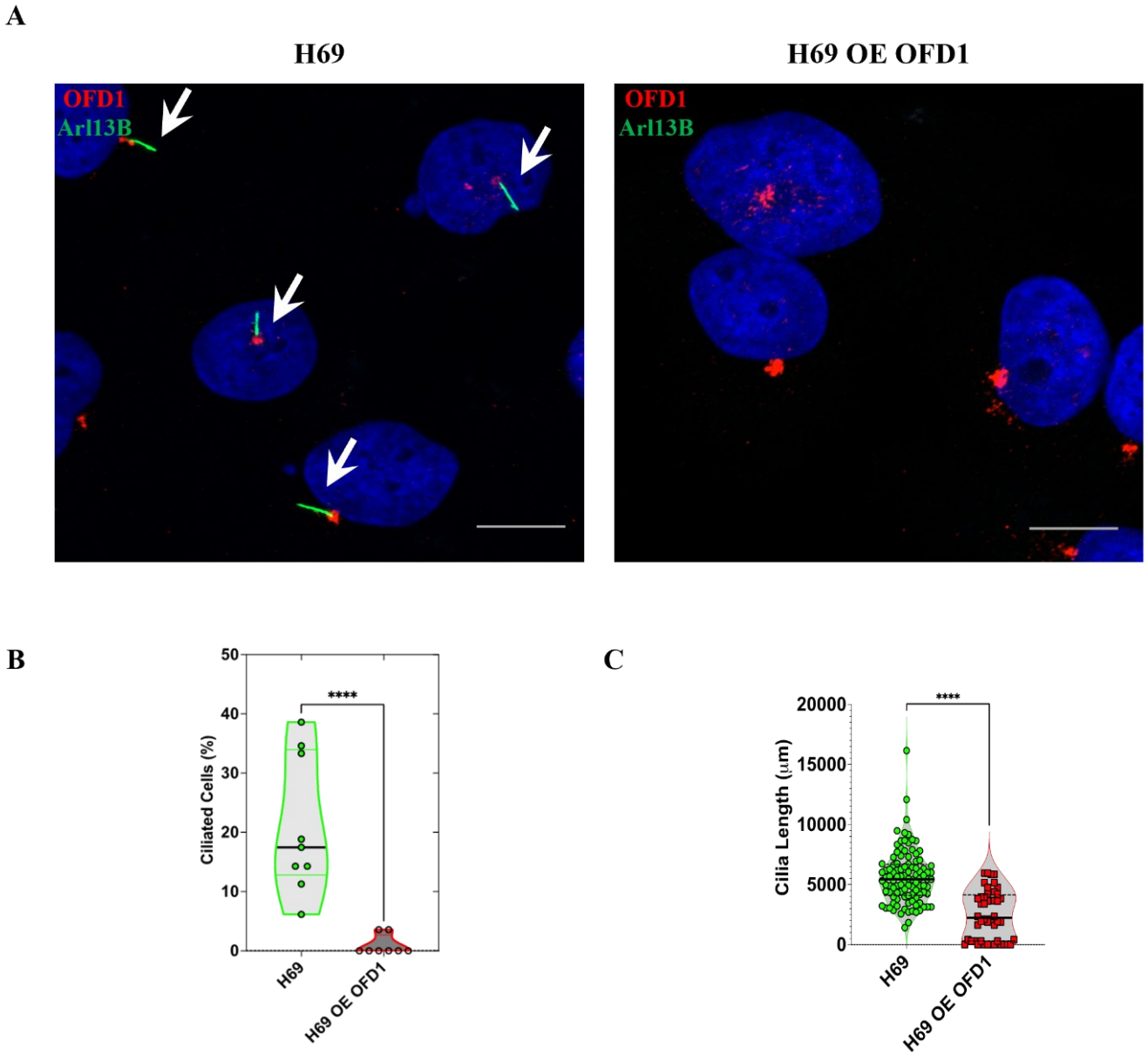

Figure 14. OFD1 overexpression causes a significant reduction in cilia formation and length.

Immunofluorescence staining on H69 OE OFD1 cells performed after 24h starvation. H69 wild-type cell line was used as control. Double immunostaining of anti-Arl13b (green), showing primary cilia (arrow) and anti-OFD1 (red) shown. Nuclei were stained with DAPI (blue). Scale bars are equal to 20 µm (**A**). Quantitative analysis of ciliated cells and cilia length were performed by using ImageJ Software (**B**, **C**). ****$p < 0.00001$.

To further corroborate the impact of OFD1 overexpression on ciliogenesis, we assessed the expression levels of acetylated tubulin, an axonemal marker, in H69 OE OFD1 cells and control. By performing Western Blot analysis, we observed that OFD1 overexpression decreased the expression levels of acetylated tubulin, thus confirming a substantial loss of primary cilia (Fig. 15). In fact, the level of expression of OFD1

increased in protein lysate from H69 OE OFD1 cells confirming the overexpression, while the acetylated tubulin is clearly highly expressed in H69 cells respect to H69 OE OFD1 cells (Fig. 15).

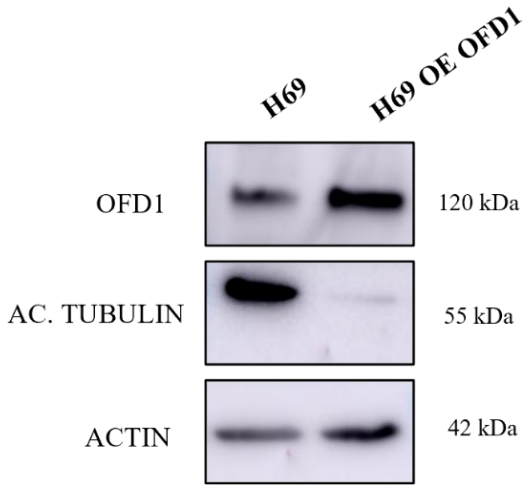

Figure 15. OFD1 overexpression affects ciliary proteins expression.

Western blot analysis was performed on H69-OFD1 overexpressing cells to evaluate the impact of OFD1 expression on the levels of the ciliary protein acetylated tubulin, H69 wild-type cells were used as control.

2.2 OFD1 overexpression promotes cell proliferation and migration in healthy human cholangiocytes

Aiming to investigate the role of OFD1 as pro-tumoral gene, we next assessed the effect of forced OFD1 overexpression on cell proliferation and migration in healthy human cholangiocyte H69 cells. To evaluate the impact of OFD1 on cell growth, we performed a colony formation assay using H69 OE OFD1 and H69 wild-type cells. Cells were plated and cultured for at least 7 days. Then, we stained the colonies with the Crystal Violet solution before counting, using a dedicated software. H69 OE OFD1 cells exhibited a significant increase in colony number compared to control cells (Fig. 16A-B). The pro-proliferation role of OFD1 was further confirmed through a (3-(4,5-dimethylthiazol-2-yl)-5-(3-carboxymethoxyphenyl)-2-(4-sulfophenyl)-2H-tetrazolium) (MTS) assay conducted on the same cell lines. This experiment demonstrated a marked increase in cell proliferation in OFD1-overexpressing cells, particularly at the lowest cell density tested (Fig. 16C).

Additionally, to gain insight into the molecular mechanism underlying the OFD1 pro-proliferative role, we assessed whether OFD1 overexpression may affect the cell cycle. For this purpose, we performed propidium iodide (PI) staining on OFD1-overexpressing H69 cells following serum starvation, using wild-type H69 cells as control. Flow cytometry (FACS) analysis revealed that OFD1 overexpression led to a decrease in the number of cells in G0/G1 phase from 90% to 80% and, at the same time, a significant increase in the percentage of ciliated cells in G2/M phase, from 3% to 10%, compared to control cells, indicating that OFD1 overexpression promotes mitotic rate and cell division (Fig. 16D-E).

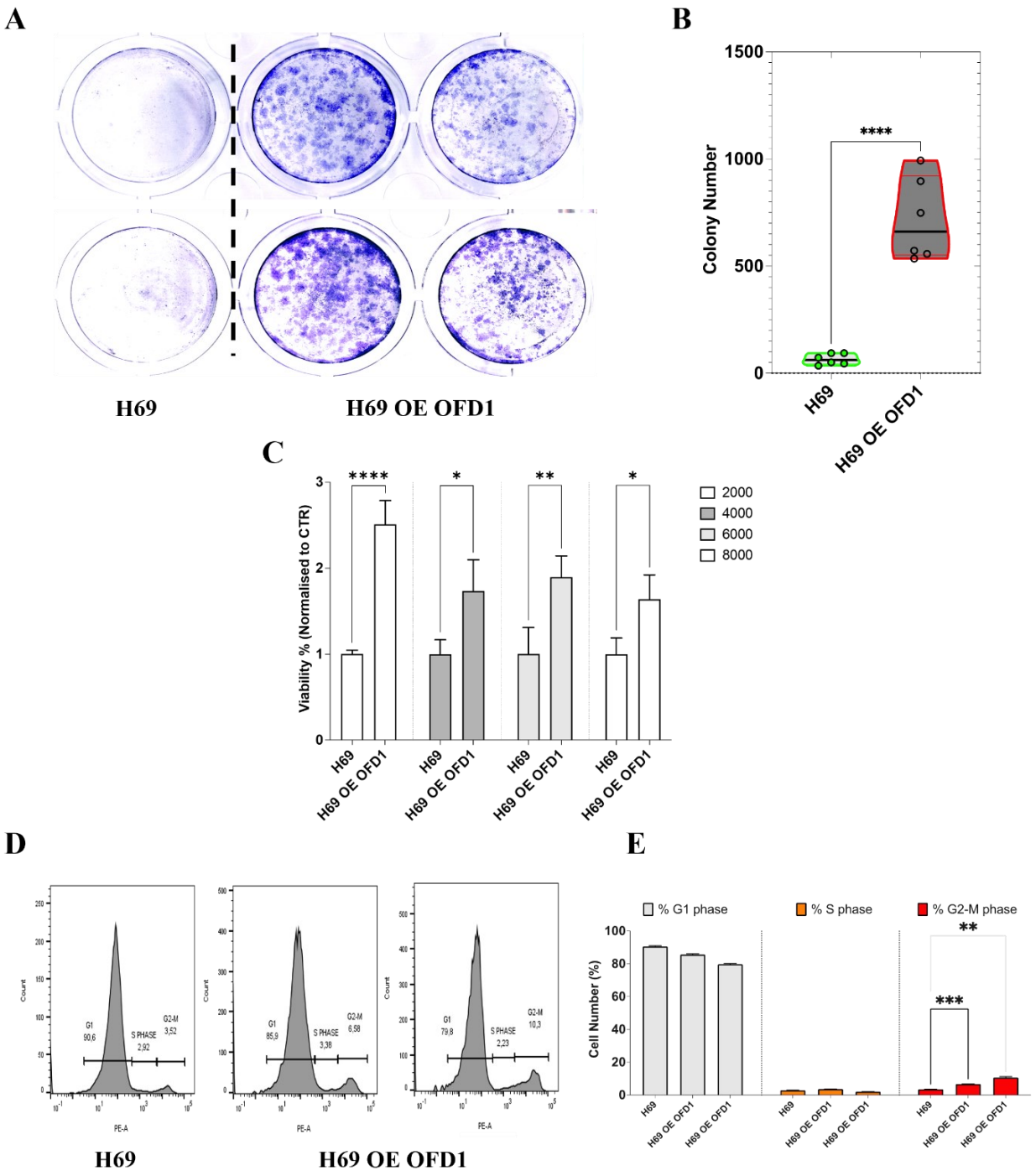

Figure 16. OFD1 overexpression promotes cell proliferation in H69 cell line.

H69 OE OFD1 cells were plated at low density in 24-well plate. H69 wild-type cell line was used as control. After 8 days, cells were stopped, and Crystal Violet staining was performed. Colony count was performed by using ImageJ Software (**A**, **B**). H69 OE OFD1 were plated at different number of cells/well in 96-well plate. H69 wild-type cell line was used as control. Cells were starved for 24h, after starvation complete media was replaced. Cell proliferation was assessed after 48h (**C**). FACS Analysis on H69 OE OFD1 cells. Propidium Iodide (PI) staining was performed. H69 wild-type cell line was used as control. Cells were starved overnight; complete medium was replaced by 48h (**D**, **E**). *p < 0.01; **p < 0.001; ***p < 0.0001; ****p < 0.00001.

Moreover, we evaluated the effect of OFD1 on cell migration by performing a wound healing assay. This assay is commonly used to study cell migration in cell culture. The

analysis revealed that H69 OE OFD1 cells exhibited increased migration compared to control cells, completely filling the scratch after 48 hours (Fig. 17). Our results showed that substantial differences were found in the wound area at 24h and 48h, indicating that OFD1 may influence cell migration. Collectively, these findings suggest that OFD1 may have an oncogenic effect on healthy human cholangiocytes by promoting both cell proliferation and migration.

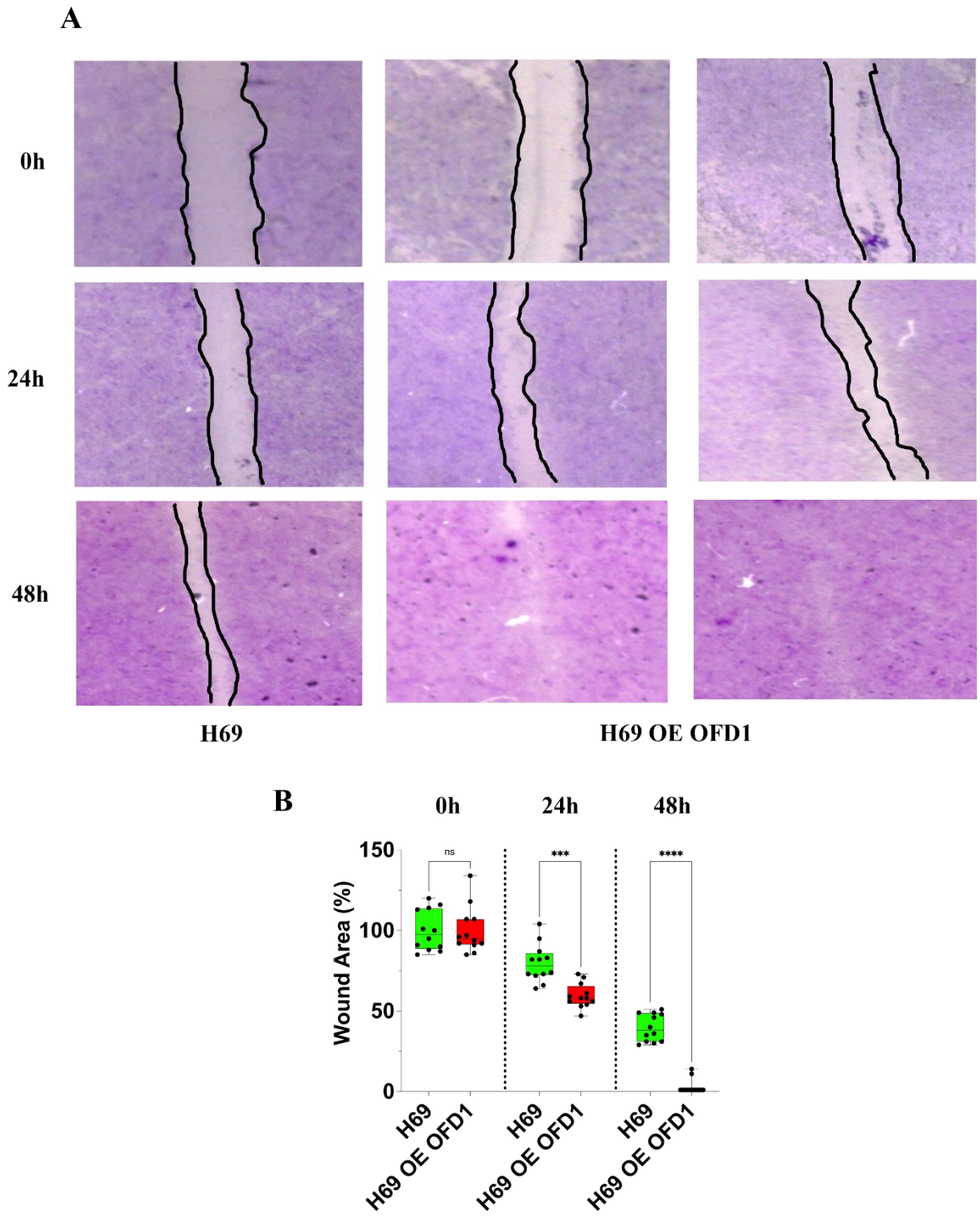

Figure 17. OFD1 impact on cell migration.
Wound healing assay performed on H69 OE OFD1 cells. H69 wild-type cells were used as control. Cell migration was evaluated at three different time points. Wound area measurement was performed by using ImageJ Software (**A, B**). ***$p < 0.0001$; ****$p < 0.00001$; ns, not significative.

2.3 OFD1 depletion induces cilia formation in CCA cell line

To further confirm the central role of OFD1 in regulating primary cilium biogenesis in CCA cells, we investigated its involvement in ciliogenesis using the intrahepatic CCA (iCCA) cell line RBE. We first evaluated the effect of OFD1 forced downregulation on cilia formation. To this aim, we performed OFD1 forced downregulation in RBE cells by transiently transfecting with small interfering RNA (siRNA) against OFD1 (RBE OFD1-KD) and performed an immunofluorescence experiment. We used an antibody labelling OFD1 to confirm the significant downregulation of the protein (up to 100% after 72h transfection) and an antibody labelling ARL13B as previously described for H69 cells. As shown in Fig. 18A, no cilia were observed in control cells, as expected, whereas OFD1 downregulation led to an increased presence of cilia on the cell surface. Western blot analysis of various ciliary proteins in RBE OFD1-KD and control cells was consistent with the immunofluorescence findings, showing increased expression levels of ciliary proteins in OFD1-downregulated cells compared to controls. The analyzed ciliary protein markers were pericentriolar material 1 protein (PCM1), representative for the basal body, intraflagellar transport proteins 88 and 20 (IFT88 and IFT20) both involved in protein trafficking within the cilium, ARL13B and acetylated tubulin as axonemal markers. Our results showed that the OFD1 levels were completely downregulated by the siRNA used in our experiment. On the other hand, the OFD1 forced downregulation was responsible for the increased expression of all the ciliary markers mentioned before (Fig. 18B).

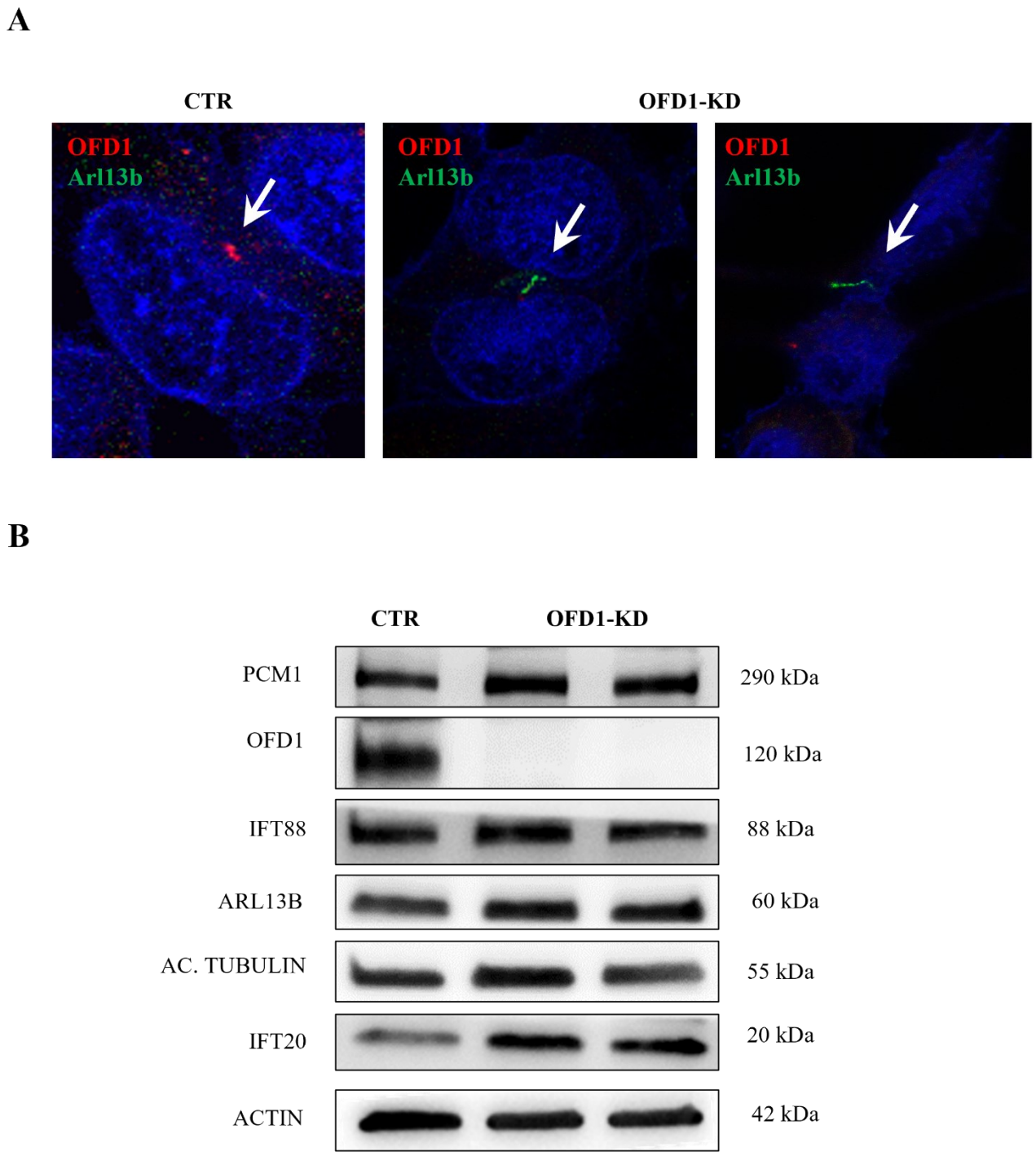

Figure 18. OFD1 Knock-down induces cilium formation in CCA cell line RBE.
RBE cell line was transfected with siRNA CTR and OFD1 siRNA and then immunofluorescence staining was performed after 24h starvation. White arrows indicate primary cilia. Representative images in Fig. (**A**). Western blot Analysis was performed to evaluate OFD1 impact on ciliary proteins expression (PCM1, IFT88, ARL13B, acetylated tubulin and IFT20) in RBE OFD1-KD cells and control (**B**).

To confirm these findings, we used CRISPR/Cas9 gene editing to deplete OFD1 in RBE cells. Specifically, we generated an OFD1 knockout RBE cell line (RBE KO OFD1) using a lentiviral-based CRISPR/Cas9 system. To validate the genome editing,

we performed Real Time and Western blot analysis. As shown in Fig. 19A-B, significant changes in OFD1 mRNA levels were observed and a complete knockout at the protein level was confirmed.

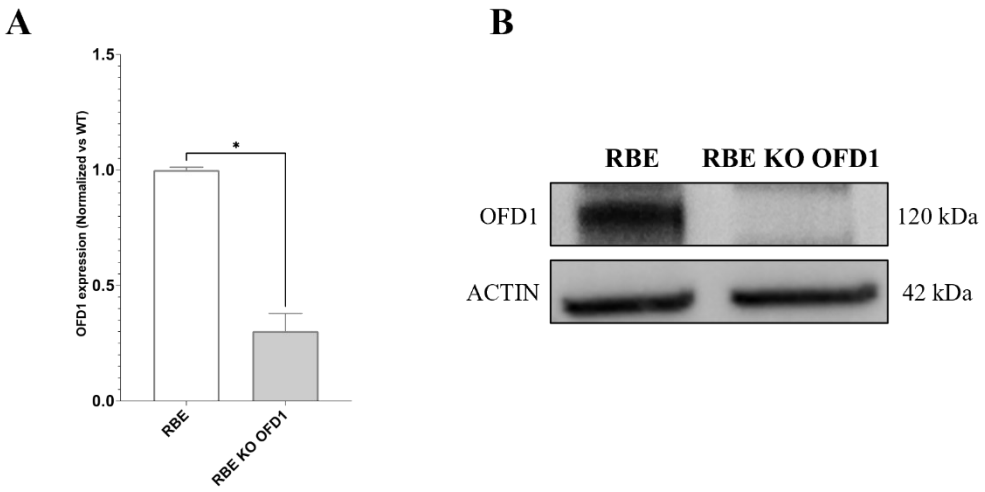

Figure 19. Generation of RBE KO OFD1 cell line.

The RBE cell line was transfected with plasmid carrying CRISPR/Cas9 system. OFD1 mRNA expression analysis using RT-PCR in RBE KO OFD1 cells. RBE wild-type cell line was used as relative control (**A**). *$p < 0.01$. Western blot analysis for OFD1 of protein lysates obtained from RBE wild-type and RBE KO OFD1. ACTIN was used as loading control (**B**).

Next, immunofluorescence staining was performed to further investigate the role of OFD1 in modulating cilia biogenesis in CCA cells. We used an antibody labelling OFD1 to confirm the depletion and an antibody labelling ARL13B as previously described for the other immunofluorescence experiments. Notably, in RBE KO OFD1 cells the complete depletion of OFD1 restored ciliogenesis. In fact, in this cell line an increased number of ciliated cells was shown (Fig. 20).

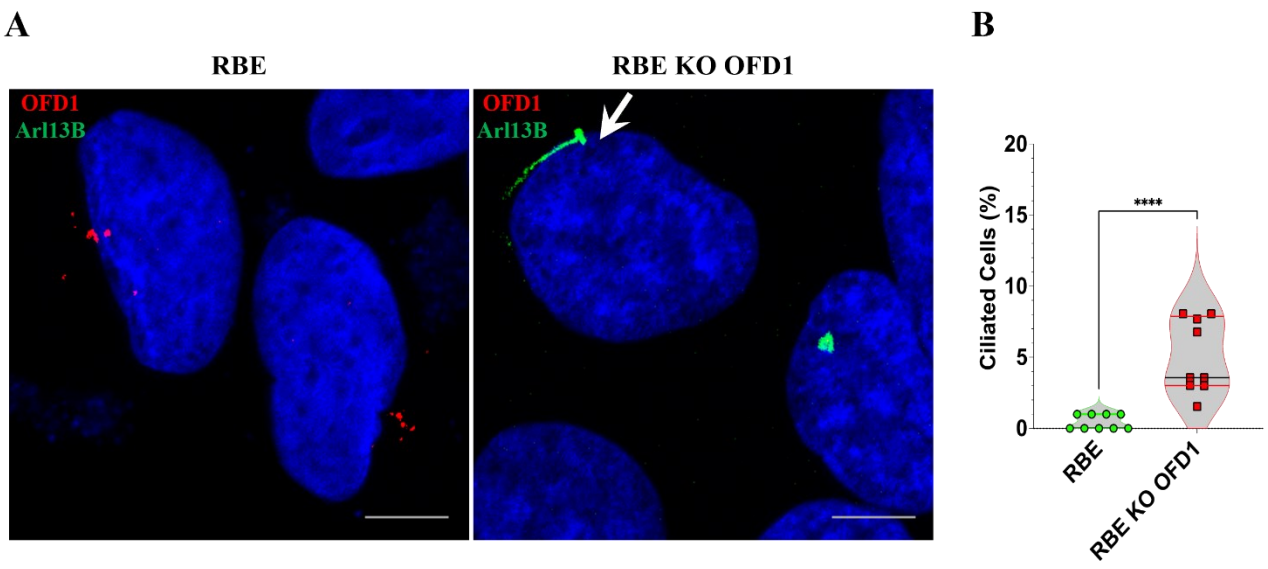

Figure 20. OFD1 depletion restores ciliogenesis in RBE cell line.
Immunofluorescence staining on RBE KO OFD1 cells was performed after 24h starvation. RBE wild-type cells were used as control. Double immunostaining of anti-Arl13b (green) and anti-OFD1 (red). Nuclei were stained with DAPI (blue). Scale bars are equal to20 µm (**A**). Quantitative analysis of ciliated cells and cilia length were performed by using ImageJ Software (**B**). ****$p < 0.00001$.

2.4 OFD1 depletion reduces cell proliferation and migration in CCA cell line

To further define the pro-oncogenic role of OFD1 in CCA, we investigated how OFD1 modulation affects cell proliferation in the RBE cell line through a series of *in vitro* experiments. First, we performed a colony formation assay to determine whether OFD1 depletion reduces cell proliferation. As shown in Fig. 21A-B, the depletion of OFD1 resulted in a significant reduction in the number of colonies compared to control cells. Next, we evaluated the impact of OFD1 knockout using an MTS assay. Analysis of absorbance measurements revealed a marked decrease in cell growth in RBE KO OFD1 cells compared to control cells (Fig. 21C).

Finally, to confirm the impact of OFD1 depletion on cell proliferation, we conducted a FACS analysis using PI staining to study the cell cycle. PI staining was performed on RBE KO OFD1 cells after serum starvation, with RBE wild-type cells used as controls. Our FACS analysis revealed that OFD1 depletion resulted in an increased number of cells in the S phase and a marked reduction in the G2/M phase compared to

control cells. These findings indicate that OFD1 knockout causes a delay in cell cycle progression, likely due to an impairment during G1/S transition (Fig. 21D-E).

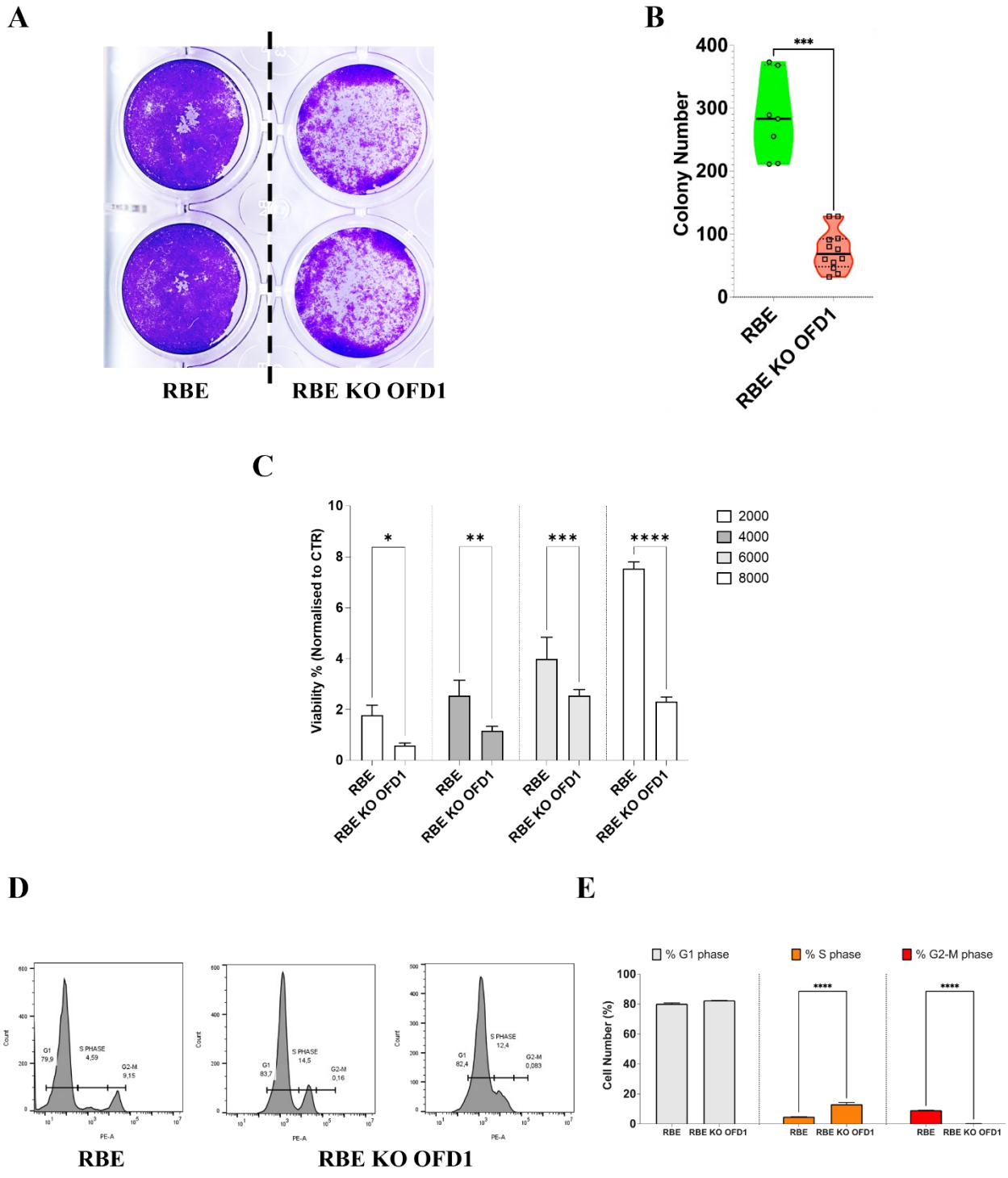

Figure 21. OFD1 knockout reduces cell proliferation in RBE cells.

RBE KO OFD1 cells were plated at low density in 24-well plate. RBE wild-type cell line was used as control. After 8 days, cells were stopped, and Crystal Violet staining was performed. Colony count was performed by using ImageJ Software (**A**, **B**). RBE KO OFD1 cells were plated at different number of cells/well in 96-well plate. RBE wild-type cell line was used as control. Cells were starved for 24h, after starvation complete media

was replaced. Cell proliferation was assessed after 48h (**C**). Cell Cycle analysis by FACS on RBE KO OFD1 cells. RBE wild-type cell line was used as control. Propidium Iodide (PI) staining was performed. RBE wild-type cell line was used as control. (**D**, **E**). *p < 0.01; **p < 0.001; ***p < 0.0001; ****p < 0.00001.

Furthermore, we assessed the impact of OFD1 on cell migration using a wound healing assay. The analysis revealed that RBE KO OFD1 cells exhibited reduced migration compared to control cells (Fig. 22). Significant differences in the wound area were observed at 24 and 48 hours, suggesting that OFD1 depletion may impair cell migration. These findings align with previously reported results in the H69 OE OFD1 cell line and further support our hypothesis that OFD1 influences cell migration. Collectively, these findings suggest that OFD1 may have an oncogenic role in CCA cell lines.

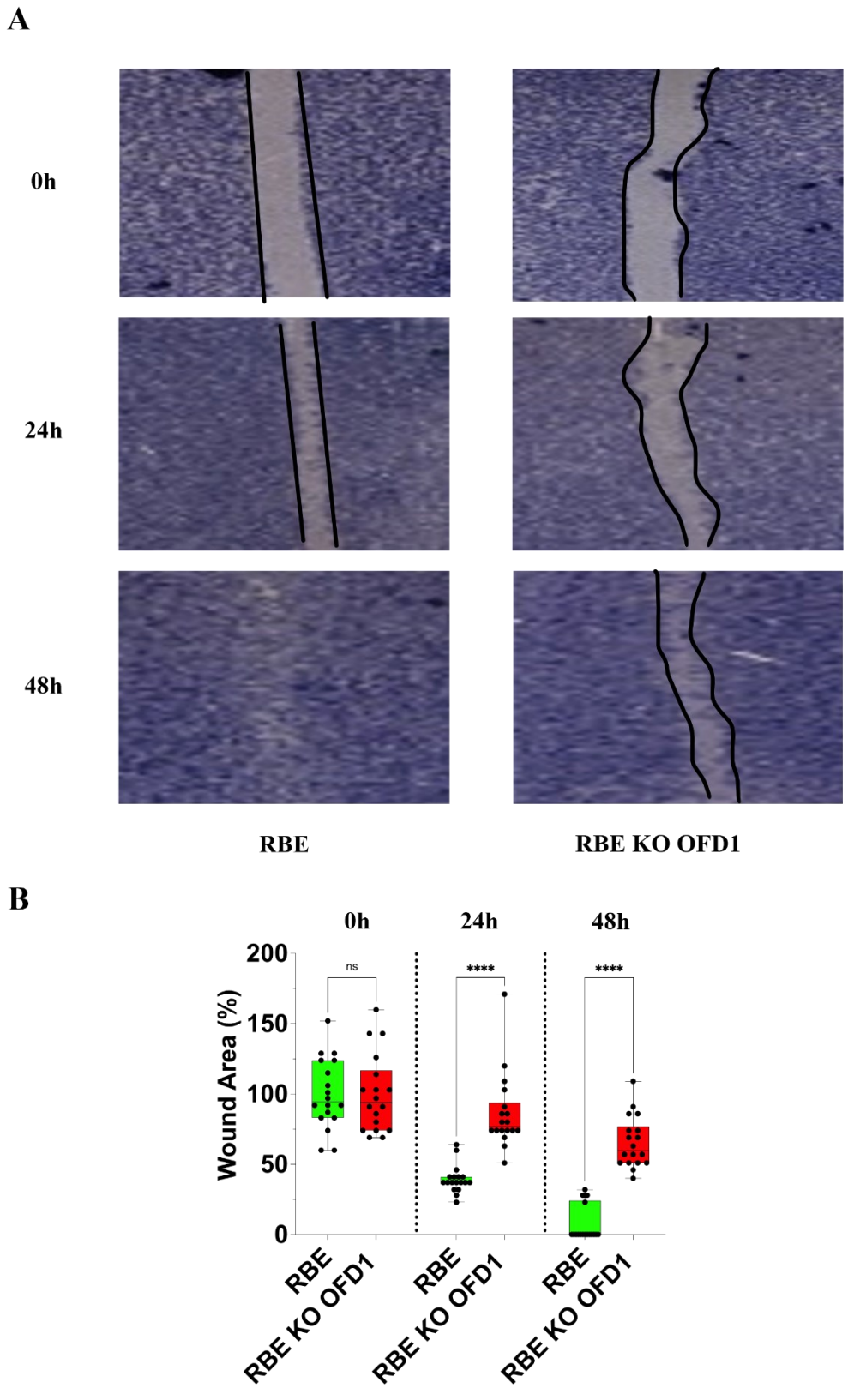

Figure 22. OFD1 depletion reduces cell migration.

Wound healing assay performed on RBE KO OFD1 cells. RBE wild-type cells were used as control. Cell migration was evaluated at three different time points. Wound area measurement was performed by using ImageJ Software (A, B). ****$p < 0.00001$; ns, not significative.

3. OFD1-High expression is associated with poor prognosis in CCA patients

We previously demonstrated that OFD1 is overexpressed in CCA and assessed the potential role of OFD1 as oncogene in several cell models and different approaches (see Figs. 16-17-21-22).

At this point, we investigated if the oncogenic role of OFD1 may have clinical relevance in CCA patients. Our cohort of 80 patients was divided into two groups based on the levels of expression of OFD1: high-OFD1 (high expression) and low-OFD1 (low expression). We assessed the Overall Survival (OS) rate and observed that patients with high OFD1 expression had a significantly shorter survival probability compared to those in the low-OFD1 group (OS 10 vs 39 months; HR 2.33, 95% CI 1.01–5.31, $p < 0.05$), suggesting that OFD1 may play a role in promoting tumor progression (Fig. 23).

Currently, one of the main problems in CCA is the lack of specific biomarkers that enable early-stage diagnosis. Considering our transcriptomic analysis, *in vitro* experiments, and the observed correlation between OFD1 expression and clinical prognosis, these findings provide new insights into the potential use of OFD1 as a biomarker for the clinical management of CCA patients.

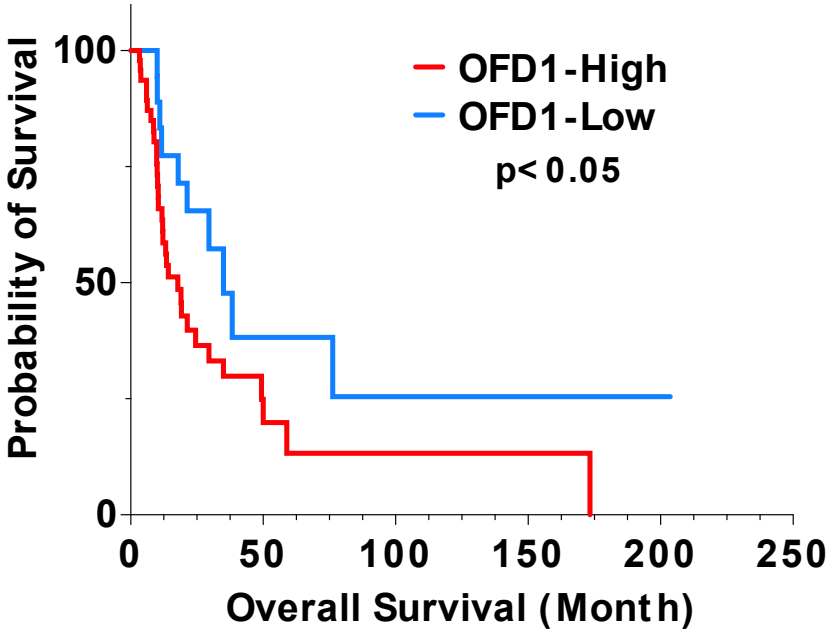

Figure 23. Clinical relevance of OFD1 in CCA patients.

Kaplan–Meier estimating Overall Survival (OS) of patients with high and low OFD1 expression. Patients were stratified by medians into OFD1-Low and OFD1-High groups. Pairwise log-rank test was used to analyze survival; $p < 0.05$.

Discussion

Currently, little is known about the functional interplay between primary cilia and cholangiocarcinoma (CCA), and the mechanisms underpinning this relationship remain unclear. The primary cilium is a non-motile cellular organelle essential for normal development and tissue homeostasis[49]. Structurally, it resembles an antenna-like projection extending from the surface of most mammalian cells. It consists of three main components: (1) the basal body, derived from the differentiation of the mother centriole of the centrosome, (2) the transition zone, which acts as a gate controlling the entry and exit of cargo within the cilium, and (3) the axoneme, a cytoskeletal structure formed by nine doublets of microtubules surrounded by the ciliary membrane[43,50]. It is well established that mutations impairing primary cilia biogenesis, structure, or function can disrupt signaling pathways, leading to non-motile ciliopathies—a group of more than 30 human diseases and syndromes that affect multiple tissues and organs, including the eye, kidney, liver, brain, skeleton, and heart[52–54].

Over the past few decades, the primary cilium has emerged as a key organelle in carcinogenesis[58]. Acting as a signaling hub, the primary cilium mediates the reception and transmission of extracellular signals, thereby regulating essential biological processes such as development, differentiation, growth, and metabolism[49,54]. Recent technological advances, including various omics approaches, have provided detailed insights into primary cilia and ciliary genes in different solid tumors[58,60]. These findings suggest that the primary cilium may play a pivotal role in cancer progression[59,60]. Specifically, mounting evidence indicates that protein kinases involved in post-translational modification of ciliary proteins, intraflagellar transport proteins, and centrosomal proteins regulate critical cancer-related processes, including mitosis, DNA damage repair, and autophagy[51,56,60,69]. Furthermore, in many solid malignancies—including pancreatic, breast, melanoma, cholangiocarcinoma, glioblastoma, prostate, and ovarian cancers—primary cilia are reduced or entirely

absent in tumor cells, supporting the hypothesis that the primary cilium functions as a tumor suppressor organelle[59].

CCA is a rare and aggressive malignancy originating from the transformation of epithelial cells lining the biliary ducts[1,2]. It includes several subsets of biliary cancers arising along the biliary tree, which differ in histopathology and molecular alterations[3,4]. The current classification distinguishes three main subtypes based on anatomical location: distal (dCCA), perihilar (pCCA), and intrahepatic (iCCA)[1,2]. CCA is often asymptomatic in its early stages, and due to the lack of specific symptoms and biomarkers, it is typically diagnosed at advanced stages[41]. Additionally, its incidence and mortality are increasing globally[34].

Regarding therapeutic approaches, the gold standard remains surgical resection when feasible, followed by chemotherapy combined with immunotherapy or, in advanced cases, palliative systemic chemotherapy[41]. However, a major challenge lies in the highly heterogeneous genetic background of CCA, which currently precludes the development of effective targeted therapies[19–21].

Consequently, the scientific community has dedicated significant effort to discovering novel druggable targets to enable more effective therapeutic strategies. Evidence in the literature highlights a reduction or complete loss of primary cilia in CCA. Indeed, experimental evidence have demonstrated that in CCA cell lines representing the three main subtypes—dCCA, pCCA, and iCCA—the presence of primary cilia on the cell surface is markedly reduced or completely absent compared to normal, healthy epithelial cholangiocytes. However, the mechanisms underlying this phenomenon remain poorly understood[59].

The study described in this thesis aims to investigate ciliary genes and primary cilia dysfunction in CCA, with the ultimate goal of identifying and functionally characterizing cilia-associated genes that hold potential translational relevance for CCA prognosis and treatment.

In this context, we studied the expression of genes associated with the primary cilium, collectively referred to as the *Ciliome*, in a cohort of 80, clinically annotated, CCA

patients. Whole-transcriptome profiling was performed on laser micro-dissected formalin-fixed, paraffin-embedded (FFPE) tissue specimens. Differential gene expression (DEG) analysis was conducted by comparing tumor, stromal, and normal tissue areas taking advantage of spatial transcriptomic studies. The identified DEGs were cross-referenced with the Cilia Carta database to isolate dysregulated ciliary genes.

This analysis focused on the expression levels of genes involved in ciliogenesis and cilia structure, such as axonemal and basal body genes, as well as cilia-associated genes, including those encoding proteins involved in the post-translational modifications of ciliary proteins. Our results allowed us to demonstrate that ciliary genes were significantly dysregulated in CCA tumor tissues compared to normal tissues. Among ciliary genes, bioinformatic analysis revealed that *OFD1* was one of the most altered genes in tumor area.

OFD1 stands for Orofacial-Digital-Syndrome type 1 protein, the name of the genetic syndrome which rises from OFD1 alteration[71]. *OFD1* is located on the X chromosome and is essential for primary cilia formation[75]. While it is well established that mutations in *OFD1* cause ciliopathies[82,83], its role in cancer remains poorly understood. However, evidence from the literature has shown that OFD1 is highly expressed in oropharyngeal squamous cell carcinoma (OPSCC) and endometrial cancer[89,90], though the mechanisms underlying its dysregulation in these cancers are still under investigation. We found for the first time OFD1 dysregulation also in CCA. Previous reports together with our transcriptomic profiling showing the overexpression of OFD1 in tumor samples led us to hypothesize that OFD1 may act as an oncogene in CCA.

To further corroborate our hypothesis, we assessed the impact of OFD1 on ciliogenesis in a wild -type human cholangiocyte cell line (H69) overexpressing the OFD1 transcript (H69 OE OFD1). Healthy human cholangiocytes are known to express primary cilia on their surface. Our results demonstrated that OFD1 overexpression caused a marked reduction in primary cilia formation, whereas in the wild-type counterpart, primary cilia were consistently present on the cell surface. Additionally, a

significant reduction in cilia length was observed in OFD1-overexpressing cells compared to the control.

To further characterize the phenotype of H69 OFD1-overexpressing cells, we investigated whether OFD1 upregulation might be associated with alterations in cell proliferation. Evidence from the literature has demonstrated that alterations in ciliary genes can influence the regulation of cell growth[58,60,90]. Confirming these results, *in vitro* assays revealed that forced OFD1 overexpression led to a marked increase in cell proliferation. Specifically, FACS analysis indicated that cells with high OFD1 expression exhibited an increase in the G2/M phase and a significant decrease in the G0/G1 phase. These findings suggest that H69 OE OFD1 cells were more prone to division and proliferation compared to control cells.

Moreover, previous studies have suggested that alterations in ciliary genes can influence cell migration[63]. Based on this, we evaluated whether OFD1 overexpression and depletion affected cell migration in our cellular model. Interestingly, our results showed a substantial increase in cell migration in the H69 cell line with forced OFD1 overexpression compared to the control, whereas OFD1 depletion significantly reduced cell migration in the RBE cell line (a cholangiocarcinoma cell line) when compared to controls.

To further confirm the role of OFD1 as a potential oncogene in CCA, we investigated the impact of OFD1 depletion on cell proliferation in CCA cells. Previous studies have shown that mutations in OFD1 can lead to lower proliferation rates and cell cycle progression defects, resulting in G2/M phase arrest in fibroblasts[79]. Our *in vitro* experiments on RBE KO OFD1 cells demonstrated that OFD1 depletion significantly reduced cell proliferation. This was further corroborated by our FACS analysis, which revealed that RBE KO OFD1 cells exhibited an accumulation of cells in S phase and, simultaneously, a marked block in G2/M phase. Taken together, our data suggest that alterations in OFD1 expression can lead to delays in the cell cycle, resulting in reduced cell proliferation in CCA cells.

Finally, to confirm our hypothesis that OFD1 could serve as a potential biomarker in CCA, we evaluated its clinical relevance and association within the CCA patient cohort included in our study. To this end, patients were stratified into two groups based on OFD1 expression: OFD1-High and OFD1-Low. An overall survival analysis was performed, and the resulting Kaplan-Meier curve demonstrated that the OFD1-High group had a significantly lower survival rate compared to the OFD1-Low group. These findings suggest that OFD1 could be a potential biomarker candidate in CCA.

Although our *in vitro* experimental data demonstrate a significant impact of OFD1 on the regulation of cell growth and cilia formation in both healthy human cholangiocytes and CCA cell lines, we cannot yet conclude whether this phenomenon is specifically related to increased OFD1 expression levels or alterations in cilia length. To address this question, future experiments will employ drugs known to modulate cilia length, enabling a more comprehensive understanding of the underlying mechanisms.

In addition, transcriptomic profiling studies will be conducted on H69 OE OFD1 and RBE KO OFD1 cell lines under serum-deprived conditions to stimulate cilia biogenesis. These transcriptomic analyses will provide deeper insights into the mechanisms driving OFD1 overexpression and identify the downstream signaling pathways it may influence.

Furthermore, xenograft mouse models will be established by injecting OFD1-modified cell lines to evaluate tumor growth *in vivo*, thereby confirming the oncogenic role of OFD1 observed in our *in vitro* experiments. These integrated approaches will enhance our understanding of OFD1's contribution to tumor biology and its potential as a novel biomarker in CCA. In conclusion, the work carried out during my PhD training enabled us to identify a novel genetic signature associated with cilium-related genes, with the *OFD1* gene emerging as the most dysregulated. Our findings identify OFD1 as a potential novel oncogene and biomarker candidate in CCA, thereby opening new therapeutic avenues and new strategies for managing CCA patients.

Materials & Methods

Human samples

The human CCA tissues were collected under approval of the Ethical Committee for Clinical Research at Azienda Ospedaliera Universitaria, Modena, Italy (ID 465/2018/SPER/AOUMO). The study protocols conformed to the ethical guidelines of the 1975 Declaration of Helsinki, as per ethical approval given by the institutional review board. Written informed consent was obtained from all participants. Diagnosis of CCA was established on radiological findings and was pathologically proven in all patients. Inclusion Criteria, Subject Demographics, Sex and Biological Variables and Clinicopathological characteristics were shown in Fig. 11. Disease recurrence was defined as the presence of imaging-proven disease. Total RNA was extracted from the Formalin-Fixed-Paraffin-Embedded (FFPE) samples from 80 tumors and the matched nontumor component after microscopic dissection. RNAs were extracted from FFPE tissues through Maxwell® RSC RNA FFPE Kit (Promega, Madison, WI, USA) and processed with Maxwell® RSC Instruments (Promega, Madison, WI, USA) according to the manufacturer's instructions.

Cell culture and transfections

RBE cells were obtained from DSMZ (Braunschweig, Germany) and cultured in DMEM and RPMI 1640 medium (Invitrogen, Karlsruhe, Germany) with L-Glutamine, 10% fetal bovine serum (FBS; Invitrogen, Carlsbad, CA, USA), 100 U/mL penicillin and 50 µg of streptomycin, at 37 °C in humidified 5% CO2 atmosphere. H69 cells (obtained by Lonza, Siena, IT), an SV40-transformed (i.e. immortalized) normal human cholangiocyte cell line were grown in media containing DMEM/F12 (Sigma-Aldrich, St. Louis, MO) supplemented with 10% fetal bovine serum (FBS; Invitrogen, Carlsbad, CA, USA), 100 U/mL penicillin and 50 µg of streptomycin, at 37 °C in humidified 5% CO2 atmosphere. Authentication of cell lines was done by Eurofins (Milan, Italy) and confirmed by online STR-matching analysis (www.dsmz.de/fp/cgi-bin/str.html). SiRNA against OFD1, and siRNA control were purchased from

Dharmacon (Lafayette, CO, USA). Transfection with 50 nM siRNA against OFD1 and siRNA control was performed with Lipofectamine 2000 reagent (Invitrogen, Karlsruhe, Germany).

Generation of stable cell lines

RBE KO OFD1 clone: RBE cells were transfected with an all-in-one vector containing the sgRNA of interest (target site sequence: TTAGTCCAACATGTTTACCG with predicted no off-target sites), whose expression was driven by the U6 promoter, a recombinant form of Cas9 protein under the control of the CMV promoter and an mCherry reporter gene under the control of the SV40 promoter (Genecopoeia). Cells were transfected with Lipofectamine CRISPRMAX Cas9 Transfection Reagent (Invitrogen, Thermo Fisher Scientific) according to manufacturer's instructions. Forty-eight hours after transfection, putative positive clones were FACS sorted for mCherry expression using the BD FACS Aria flow cytometer. Sorted cells were kept in culture until confluence and RT-PCR and Western blot analysis were performed to check gene editing and select clones.

H69 OE OFD1 clones: Wild-type OFD1 sequence was cloned into pDONR223 vector using the BP Clonase Reaction Kit (Invitrogen) and further recombined into the doxycycline inducible lentiviral GATEWAY destination vector pLVX using In Fusion Cloning kit (Takara). Primers were designed following the indication available at https://www.takarabio.com/products/cloning/in-fusion-cloning. Stable and inducible cell lines were generated using the produced lentiviral plasmids. Virus was produced in HEK 293T cells and HK2/HEK293 cells were infected for 48hr before selection with puromycin.

RNA extraction and Real-Time PCR

Total RNA was extracted from the cell samples using Trizol reagent (Invitrogen, California, CA, USA) or in alternative Maxwell RSC simplyRNA Cells (Glomax Discover System, Promega, Madison, WI, USA) and processed with Maxwell RSC Instrument (Glomax Discover System, Promega, Madison, WI, USA) following manufacturer's instructions [21]. Single-stranded complementary DNA (cDNA) was generated using High Capacity cDNA Reverse Transcription Kit (Life Technologies, Paisley, UK). Real-Time PCR (RT-PCR) was performed in LightCycler 96 (Roche, Penzberg, Germany) using LightCycler FastStart DNA Master SYBR Green I (Roche, Penzberg, Germany) and each validated primer. Validated RT-PCR primers of OFD1, GAPDH and ACTIN were purchased from Eurofins (Milan, Italy).

The primer sequences are as follows:

OFD1: REV GAGACTGGAAGTAGGGTTGATTTT; For TCTTTCCAGAAAGTGGTTTGG

GAPDH: REV AGGGGTGCTAAGCAGTTGGT; FOR ATGTTCGTCATGGGTGTGAA

ACTIN: REV GACTCCATGCCCAGGAGGG; FOR AAGAGCTACGAGCTGCCTGA

Proliferation assay

MTS assays were performed using tetrazolium-based CellTiter 96 AQueous One Solution Cell Proliferation assay (Promega, Madison, WI, USA). Cells were seeded in 96-well plates at 10,000 cells per well for overnight incubation. Following adhesion of cells to the well, cells were serum starved overnight, and then complete media was replaced. At the designated time-points, plates were read at the absorbance of 492 nm on a microplate reader (Glomax Discover System, Promega, Madison, WI, USA). Relative cell viability of an individual sample was calculated by normalizing their absorbance to that of the corresponding control. All experiments were done in

triplicate. The GI50 was determined from the regression of a plot of the logarithm of the concentration versus percent inhibition by Prism GraphPad (GraphPad Software 8.0, La Jolla, CA, USA) using the Dose–Response One-Site Model.

Colony formation assay

The cells were seeded onto 24-well plates (6000 cells/well) and serum deprived overnight. After starvation, complete medium was replaced. Cells were cultured for 7–10 days. After washing and fixation, the cells were stained with 0.5% Crystal Violet (Bio Basic Inc., Markham, Canada) in 25% methanol for 10 min. Cell colonies were then photographed and counted by using ImageJ Software.

Wound healing assay

Cells were seeded onto 12-well plates and serum deprived overnight. After starvation, scratch was performed by using a p200 tip. Low-serum medium was added to cells and wound area was evaluated at designed time-points. After washing and fixation, the cells were stained with 0.5% Crystal Violet (Bio Basic Inc., Markham, Canada) in 25% methanol for 10 min. Wound areas were then photographed and measured by using ImageJ Software.

PI staining assay

Cells were seeded onto 6-well plates and serum deprived overnight. After starvation, complete medium was replaced for 48 h, and the cell cycle was assessed by using PI Detection Kit (BD Biosciences, San Diego, CA, USA). Cells were suspended in binding buffer, stained with PI for 15 min at room temperature in dark. Cell cycle was analyzed using a BD Accuri C6 Analyzer (BD Biosciences, San Diego, CA, USA).

Western blot analysis

The cells were lysed with RIPA buffer containing protease and phosphatase inhibitors (Selleckchem). The protein concentration was tested with a BCA kit, and appropriate

amounts of protein were prepared for SDS-PAGE and then transferred to PVDF membrane (Millipore, MA, USA). The membranes were blocked for 1 h with 5% non-fat dry milk and then incubated with rabbit anti-OFD1 (1:1000; HPA031103; Sigma); ARL13B (1:1000; SC-515784; Santacruz); ACETYLATED TUBULIN (1:1000; T6793; Sigma); PCM1 (1:1000; #MA1-106; Invitrogen); IFT88 (1:1000; 13967-1-AP; Proteintech); IFT20 (1:1000; 13615-1-AP; Proteintech); ACTIN (1:5000, A5441; Sigma) mAB was used as loading controls. The results were imaged using a gel image analysis system (Bio-Rad, California, USA) according to the manufacturer's instructions.

Immunofluorescence

Cells were grown on glass coverslips, fixed for 5 min in cold methanol and permeabilized in 0.05% (w/v) saponin, 0.5% (w/v) BSA, 50mM NH_4Cl, and 0.02% NaN_3 in PBS (blocking buffer) for 30min. Cells were incubated with primary antibodies either at 4°C overnight and then washed three times with PBS and incubated with appropriate secondary antibodies for 1h at room temperature. DNA was stained with Hoechst (33342, Sigma). After three washings with PBS, slides were mounted on coverslips with Mowiol (Calbiochem). The experiments were repeated at least three times and representative images are shown.

Confocal fluorescence microscopy and image processing

Samples were examined under LSM800 High-resolution confocal laser-scanning microscope (Zeiss). Optical sections were obtained under a 63x oil-immersion objective at a definition of 1024 X 1024 pixels, adjusting the pinhole diameter to 1 Airy unit for each emission channel. To perform quantitative image analysis, 10–15 randomly chosen fields that included 8-10 cells each were scanned, using the same setting parameters (i.e. laser power and detector amplification) below pixel saturation 96 between samples of interest and controls. Single channels from each image were converted into 8-bit grayscale images and thresholded in order to subtract background.

Counting was performed either automatically or manually using the tool available at https://imagej.nih.gov/ij/docs/guide/146-19.html. Images were processed using the ImageJ software. Single channels from each image were converted into 8-bit grayscale images and thresholded in order to subtract background. ImageJ Software was used to quantify the number of ciliated cells and primary cilia length.

RNA-Seq library preparation and deep sequencing

For RNA-Seq analysis, libraries were prepared according to the manufacturer's instructions (QuantSeq 3' mRNA-Seq Library Prep Kit FWD for Illumina, Lexogen GmbH, Wien, Austria) starting from 250 ng of total RNA. Quality control of library templates was performed using a High Sensitivity D1000 Screen Tape (Agilent Technologies, Santa Clara, CA, USA) on a TapeStation 4200 (Agilent Technologies, Santa Clara, CA, USA). The Qubit quantification platform (Qubit 2.0 Fluorometer, Life Technologies/Thermo Fisher Scientific, MA, USA) was used to normalize samples for the library preparation. Using multiplexing, up to 87 samples were combined into a single lane to yield sufficient coverage. The sequencing was carried out in collaboration with Next Generation Diagnostic S.r.l. (Pozzuoli, Naples, Italy). Libraries were sequenced by single-end chemistry on an NovaSeq6000 platform (SP 100 cycles; Illumina, Cambridge, UK). Each library was loaded at a concentration of 250 pM, which was previously established as optimal. An average yield of ~ 4.5 Mb was obtained per sample.

Computational analysis of deep sequencing data

A data analysis was performed using the pipeline already established at the Bioinformatics and Statistics Core Facility at TIGEM [16]. Briefly, the reads were trimmed to remove adapter sequences and low-quality ends and reads mapping to contaminating sequences (e.g., ribosomal RNA, phIX control) were filtered out. Reads were aligned and assigned to Human ENSEMBLE transcripts and genes (hg38

reference) by using RSEM version 1.2.25 with standard parameters. The threshold for statistical significance chosen was False Discovery Rate (FDR) < 0.05. The Gene set enrichment analysis (GSEA) was then performed restricting the output to the collection of “hallmark”, “Biocarta”, “Wikipathway”, “Reactome” and “KEGG” gene sets part of the Molecular Signatures Database (MSigDB v7.0). The threshold for statistical significance chosen in the GSEA was False Discovery Rate (FDR) < 0.25. The expression of differentially induced/suppressed genes (FDR < 0.05) was validated by RT-PCR.

Statistical analysis

Statistical tests including Student’s t test and one-way ANOVA with Bonferroni’s multiple comparison test were performed with Prism GraphPad (GraphPad Software 8.0, La Jolla, CA, USA). Data are presented as mean +/− SD. Results were considered statistically significant if $p < 0.05$. The calculation of the cell viability values were performed with Prism GraphPad Prism (GraphPad Software 8.0, La Jolla California, USA). The values were log transformed before fitting the model. 4.13. For survival data, Kaplan–Meier curves were plotted and compared using a logrank test. All tests were two-sided. All analysis was performed with R software (version 4.0.2) using survival R package. A p-value < 0.05 was considered statistically significant.

References

1. Banales, J. M. *et al.* Cholangiocarcinoma 2020: the next horizon in mechanisms and management. *Nat Rev Gastroenterol Hepatol* **17**, 557–588 (2020).
2. Banales, J. M. *et al.* Cholangiocarcinoma: current knowledge and future perspectives consensus statement from the European Network for the Study of Cholangiocarcinoma (ENS-CCA). *Nat Rev Gastroenterol Hepatol* **13**, 261–280 (2016).
3. Khan, S. A. *et al.* Guidelines for the diagnosis and treatment of cholangiocarcinoma: an update. *Gut* **61**, 1657–1669 (2012).
4. Khan, A. S. & Dageforde, L. A. Cholangiocarcinoma. *Surgical Clinics of North America* **99**, 315–335 (2019).
5. Ilyas, S. I., Khan, S. A., Hallemeier, C. L., Kelley, R. K. & Gores, G. J. Cholangiocarcinoma — evolving concepts and therapeutic strategies. *Nat Rev Clin Oncol* **15**, 95–111 (2018).
6. Brindley, P. J. *et al.* Cholangiocarcinoma. *Nat Rev Dis Primers* **7**, 65 (2021).
7. Munoz-Garrido, P. & Rodrigues, P. M. The jigsaw of dual hepatocellular–intrahepatic cholangiocarcinoma tumours. *Nat Rev Gastroenterol Hepatol* **16**, 653–655 (2019).
8. Blechacz, B., Komuta, M., Roskams, T. & Gores, G. J. Clinical diagnosis and staging of cholangiocarcinoma. *Nat Rev Gastroenterol Hepatol* **8**, 512–522 (2011).
9. Aishima, S. & Oda, Y. Pathogenesis and classification of intrahepatic cholangiocarcinoma: different characters of perihilar large duct type versus peripheral small duct type. *J Hepatobiliary Pancreat Sci* **22**, 94–100 (2015).
10. Kendall, T. *et al.* Anatomical, histomorphological and molecular classification of cholangiocarcinoma. *Liver International* **39**, 7–18 (2019).
11. Nakanuma, Y. Pathological classification of intrahepatic cholangiocarcinoma based on a new concept. *World J Hepatol* **2**, 419 (2010).
12. Field, D. T., Carpino, G., Doukas, M. & Kendall, T. J. The morphomolecular features of cholangiocarcinoma in the personalised era. *Diagn Histopathol* **30**, 237–251 (2024).
13. Sia, D. *et al.* Integrative Molecular Analysis of Intrahepatic Cholangiocarcinoma Reveals 2 Classes That Have Different Outcomes. *Gastroenterology* **144**, 829–840 (2013).
14. Isomoto, H. *et al.* Interleukin 6 upregulates myeloid cell leukemia-1 expression through a STAT3 pathway in cholangiocarcinoma cells†. *Hepatology* **42**, 1329–1338 (2005).
15. Wehbe, H., Henson, R., Meng, F., Mize-Berge, J. & Patel, T. Interleukin-6 Contributes to Growth in Cholangiocarcinoma Cells by Aberrant Promoter Methylation and Gene Expression. *Cancer Res* **66**, 10517–10524 (2006).

16. Dai, J. *et al.* Impact of bile acids on the growth of human cholangiocarcinoma via FXR. *J Hematol Oncol* **4**, 41 (2011).
17. Brivio, S., Cadamuro, M., Strazzabosco, M. & Fabris, L. Tumor reactive stroma in cholangiocarcinoma: The fuel behind cancer aggressiveness. *World J Hepatol* **9**, 455 (2017).
18. Sirica, A. E. The role of cancer-associated myofibroblasts in intrahepatic cholangiocarcinoma. *Nat Rev Gastroenterol Hepatol* **9**, 44–54 (2012).
19. Andersen, J. B. *et al.* Genomic and Genetic Characterization of Cholangiocarcinoma Identifies Therapeutic Targets for Tyrosine Kinase Inhibitors. *Gastroenterology* **142**, 1021-1031.e15 (2012).
20. Nakamura, H. *et al.* Genomic spectra of biliary tract cancer. *Nat Genet* **47**, 1003–1010 (2015).
21. Zou, S. *et al.* Mutational landscape of intrahepatic cholangiocarcinoma. *Nat Commun* **5**, 5696 (2014).
22. Wu, Y.-M. *et al.* Identification of Targetable FGFR Gene Fusions in Diverse Cancers. *Cancer Discov* **3**, 636–647 (2013).
23. Salati, M. *et al.* The Evolving Role of FGFR2 Inhibitors in Intrahepatic Cholangiocarcinoma: From Molecular Biology to Clinical Targeting. *Cancer Manag Res* **Volume 13**, 7747–7757 (2021).
24. Farshidfar, F. *et al.* Integrative Genomic Analysis of Cholangiocarcinoma Identifies Distinct IDH-Mutant Molecular Profiles. *Cell Rep* **18**, 2780–2794 (2017).
25. Kipp, B. R. *et al.* Isocitrate dehydrogenase 1 and 2 mutations in cholangiocarcinoma. *Hum Pathol* **43**, 1552–1558 (2012).
26. Jiao, Y. *et al.* Exome sequencing identifies frequent inactivating mutations in BAP1, ARID1A and PBRM1 in intrahepatic cholangiocarcinomas. *Nat Genet* **45**, 1470–1473 (2013).
27. Xue, T.-C., Zhang, B.-H., Ye, S.-L. & Ren, Z.-G. Differentially expressed gene profiles of intrahepatic cholangiocarcinoma, hepatocellular carcinoma, and combined hepatocellular-cholangiocarcinoma by integrated microarray analysis. *Tumor Biology* **36**, 5891–5899 (2015).
28. Sekiya, S. & Suzuki, A. Intrahepatic cholangiocarcinoma can arise from Notch-mediated conversion of hepatocytes. *Journal of Clinical Investigation* **122**, 3914–3918 (2012).
29. Merino-Azpitarte, M. *et al.* SOX17 regulates cholangiocyte differentiation and acts as a tumor suppressor in cholangiocarcinoma. *J Hepatol* **67**, 72–83 (2017).

30. Li, H. *et al.* Deregulation of Hippo kinase signaling in Human hepatic malignancies. *Liver International* **32**, 38–47 (2012).
31. Sugihara, T., Isomoto, H., Gores, G. & Smoot, R. YAP and the Hippo pathway in cholangiocarcinoma. *J Gastroenterol* **54**, 485–491 (2019).
32. Ilyas, S. I. *et al.* A Hippo and Fibroblast Growth Factor Receptor Autocrine Pathway in Cholangiocarcinoma. *Journal of Biological Chemistry* **291**, 8031–8047 (2016).
33. Moeini, A., Sia, D., Bardeesy, N., Mazzaferro, V. & Llovet, J. M. Molecular Pathogenesis and Targeted Therapies for Intrahepatic Cholangiocarcinoma. *Clinical Cancer Research* **22**, 291–300 (2016).
34. Bertuccio, P. *et al.* Global trends in mortality from intrahepatic and extrahepatic cholangiocarcinoma. *J Hepatol* **71**, 104–114 (2019).
35. Strijker, M. *et al.* Treatment and survival of resected and unresected distal cholangiocarcinoma: a nationwide study. *Acta Oncol (Madr)* **58**, 1048–1055 (2019).
36. Yao, K. J., Jabbour, S., Parekh, N., Lin, Y. & Moss, R. A. Increasing mortality in the United States from cholangiocarcinoma: an analysis of the National Center for Health Statistics Database. *BMC Gastroenterol* **16**, 117 (2016).
37. Khan, S. A., Tavolari, S. & Brandi, G. Cholangiocarcinoma: Epidemiology and risk factors. *Liver International* **39**, 19–31 (2019).
38. Palmer, W. C. & Patel, T. Are common factors involved in the pathogenesis of primary liver cancers? A meta-analysis of risk factors for intrahepatic cholangiocarcinoma. *J Hepatol* **57**, 69–76 (2012).
39. Clements, O., Eliahoo, J., Kim, J. U., Taylor-Robinson, S. D. & Khan, S. A. Risk factors for intrahepatic and extrahepatic cholangiocarcinoma: A systematic review and meta-analysis. *J Hepatol* **72**, 95–103 (2020).
40. Qurashi, M., Vithayathil, M. & Khan, S. A. Epidemiology of cholangiocarcinoma. *European Journal of Surgical Oncology* 107064 (2023) doi:10.1016/j.ejso.2023.107064.
41. Vogel, A. *et al.* Biliary tract cancer: ESMO Clinical Practice Guideline for diagnosis, treatment and follow-up. *Annals of Oncology* **34**, 127–140 (2023).
42. Primrose, J. N. *et al.* Capecitabine compared with observation in resected biliary tract cancer (BILCAP): a randomised, controlled, multicentre, phase 3 study. *Lancet Oncol* **20**, 663–673 (2019).
43. Satir, P. & Christensen, S. T. Overview of Structure and Function of Mammalian Cilia. *Annu Rev Physiol* **69**, 377–400 (2007).

44. Takeda, S. & Narita, K. Structure and function of vertebrate cilia, towards a new taxonomy. *Differentiation* **83**, S4–S11 (2012).
45. Sawamoto, K. *et al.* New Neurons Follow the Flow of Cerebrospinal Fluid in the Adult Brain. *Science (1979)* **311**, 629–632 (2006).
46. Shah, A. S., Ben-Shahar, Y., Moninger, T. O., Kline, J. N. & Welsh, M. J. Motile Cilia of Human Airway Epithelia Are Chemosensory. *Science (1979)* **325**, 1131–1134 (2009).
47. Lyons, R. A., Saridogan, E. & Djahanbakhch, O. The reproductive significance of human Fallopian tube cilia. *Hum Reprod Update* **12**, 363–372 (2006).
48. Little, R. B. & Norris, D. P. Right, left and cilia: How asymmetry is established. *Semin Cell Dev Biol* **110**, 11–18 (2021).
49. Mill, P., Christensen, S. T. & Pedersen, L. B. Primary cilia as dynamic and diverse signaling hubs in development and disease. *Nat Rev Genet* **24**, 421–441 (2023).
50. Kiesel, P. *et al.* The molecular structure of mammalian primary cilia revealed by cryo-electron tomography. *Nat Struct Mol Biol* **27**, 1115–1124 (2020).
51. Morleo, M. *et al.* Crosstalk between cilia and autophagy: implication for human diseases. *Autophagy* **19**, 24–43 (2023).
52. D'Angelo, A. & Franco, B. The dynamic cilium in human diseases. *Pathogenetics* **2**, 3 (2009).
53. Baker, K. & Beales, P. L. Making sense of cilia in disease: The human ciliopathies. *Am J Med Genet C Semin Med Genet* **151C**, 281–295 (2009).
54. Reiter, J. F. & Leroux, M. R. Genes and molecular pathways underpinning ciliopathies. *Nat Rev Mol Cell Biol* **18**, 533–547 (2017).
55. Waters, A. M. & Beales, P. L. Ciliopathies: an expanding disease spectrum. *Pediatric Nephrology* **26**, 1039–1056 (2011).
56. Plotnikova, O. V., Pugacheva, E. N. & Golemis, E. A. Primary Cilia and the Cell Cycle. in 137–160 (2009). doi:10.1016/S0091-679X(08)94007-3.
57. Quarmby, L. M. & Parker, J. D. K. Cilia and the cell cycle? *J Cell Biol* **169**, 707–710 (2005).
58. Fabbri, L., Bost, F. & Mazure, N. M. Primary Cilium in Cancer Hallmarks. *Int J Mol Sci* **20**, 1336 (2019).
59. Gradilone, S. A., Pisarello, M. J. & LaRusso, N. F. Primary Cilia in Tumor Biology: The Primary Cilium as a Therapeutic Target in Cholangiocarcinoma. *Curr Drug Targets* **18**, 958–963 (2017).
60. Carotenuto, P., Gradilone, S. A. & Franco, B. Cilia and Cancer: From Molecular Genetics to Therapeutic Strategies. *Genes (Basel)* **14**, 1428 (2023).

61. Lee, K. H. *et al.* Identification of a novel Wnt5a-CK1ε-Dvl2-Plk1-mediated primary cilia disassembly pathway. *EMBO J* **31**, 3104–3117 (2012).
62. Pugacheva, E. N., Jablonski, S. A., Hartman, T. R., Henske, E. P. & Golemis, E. A. HEF1-Dependent Aurora A Activation Induces Disassembly of the Primary Cilium. *Cell* **129**, 1351–1363 (2007).
63. Li, Y. *et al.* HEF1, a novel target of Wnt signaling, promotes colonic cell migration and cancer progression. *Oncogene* **30**, 2633–2643 (2011).
64. Kim, S., Lee, K., Choi, J.-H., Ringstad, N. & Dynlacht, B. D. Nek2 activation of Kif24 ensures cilium disassembly during the cell cycle. *Nat Commun* **6**, 8087 (2015).
65. Finetti, F. *et al.* The intraflagellar transport protein IFT20 controls lysosome biogenesis by regulating the post-Golgi transport of acid hydrolases. *Cell Death Differ* **27**, 310–328 (2020).
66. Ezratty, E. J. *et al.* A Role for the Primary Cilium in Notch Signaling and Epidermal Differentiation during Skin Development. *Cell* **145**, 1129–1141 (2011).
67. Yang, H. *et al.* IFT20 Mediates the Transport of Cell Migration Regulators From the Trans-Golgi Network to the Plasma Membrane in Breast Cancer Cells. *Front Cell Dev Biol* **9**, (2021).
68. Habbig, S. *et al.* NPHP4, a cilia-associated protein, negatively regulates the Hippo pathway. *Journal of Cell Biology* **193**, 633–642 (2011).
69. Johnson, C. A. & Collis, S. J. Ciliogenesis and the DNA damage response: a stressful relationship. *Cilia* **5**, 19 (2016).
70. Hezel, A. F. *et al.* Pancreatic Lkb1 Deletion Leads to Acinar Polarity Defects and Cystic Neoplasms. *Mol Cell Biol* **28**, 2414–2425 (2008).
71. de Conciliis, L. *et al.* Characterization ofCxorf5(71-7A), a Novel Human cDNA Mapping to Xp22 and Encoding a Protein Containing Coiled-Coil α-Helical Domains. *Genomics* **51**, 243–250 (1998).
72. Ferrante, M. I. *et al.* Identification of the Gene for Oral-Facial-Digital Type I Syndrome. *The American Journal of Human Genetics* **68**, 569–576 (2001).
73. Romio, L. *et al.* OFD1 Is a Centrosomal/Basal Body Protein Expressed during Mesenchymal-Epithelial Transition in Human Nephrogenesis. *Journal of the American Society of Nephrology* **15**, 2556–2568 (2004).
74. Tang, Z. *et al.* Autophagy promotes primary ciliogenesis by removing OFD1 from centriolar satellites. *Nature* **502**, 254–257 (2013).
75. Ferrante, M. I. *et al.* Oral-facial-digital type I protein is required for primary cilia formation and left-right axis specification. *Nat Genet* **38**, 112–117 (2006).

76. Morleo, M., Pezzella, N. & Franco, B. Proteome balance in ciliopathies: the OFD1 protein example. *Trends Mol Med* **29**, 201–217 (2023).
77. Singla, V., Romaguera-Ros, M., Garcia-Verdugo, J. M. & Reiter, J. F. Ofd1, a Human Disease Gene, Regulates the Length and Distal Structure of Centrioles. *Dev Cell* **18**, 410–424 (2010).
78. Abramowicz, I. *et al.* Oral-facial-digital syndrome type I cells exhibit impaired DNA repair; unanticipated consequences of defective OFD1 outside of the cilia network. *Hum Mol Genet* ddw364 (2016) doi:10.1093/hmg/ddw364.
79. Alfieri, M. *et al.* The centrosomal/basal body protein OFD1 is required for microtubule organization and cell cycle progression. *Tissue Cell* **64**, 101369 (2020).
80. Morleo, M. *et al.* Regulation of autophagosome biogenesis by OFD1-mediated selective autophagy. *EMBO J* **40**, (2021).
81. Giorgio, G. *et al.* Functional Characterization of the OFD1 Protein Reveals a Nuclear Localization and Physical Interaction with Subunits of a Chromatin Remodeling Complex. *Mol Biol Cell* **18**, 4397–4404 (2007).
82. Pezzella, N., Bove, G., Tammaro, R. & Franco, B. <scp> *OFD1* </scp> : One gene, several disorders. *Am J Med Genet C Semin Med Genet* **190**, 57–71 (2022).
83. Morleo, M. & Franco, B. OFD Type I syndrome: lessons learned from a rare ciliopathy. *Biochem Soc Trans* **48**, 1929–1939 (2020).
84. Budny, B. *et al.* A novel X-linked recessive mental retardation syndrome comprising macrocephaly and ciliary dysfunction is allelic to oral–facial–digital type I syndrome. *Hum Genet* **120**, 171–178 (2006).
85. Parisi, M. A. The molecular genetics of Joubert syndrome and related ciliopathies: The challenges of genetic and phenotypic heterogeneity. *Transl Sci Rare Dis* **4**, 25–49 (2019).
86. Webb, T. R. *et al.* Deep intronic mutation in OFD1, identified by targeted genomic next-generation sequencing, causes a severe form of X-linked retinitis pigmentosa (RP23). *Hum Mol Genet* **21**, 3647–3654 (2012).
87. Bukowy-Bieryllo, Z. *et al.* Truncating mutations in exons 20 and 21 of *OFD1* can cause primary ciliary dyskinesia without associated syndromic symptoms. *J Med Genet* **56**, 769–777 (2019).
88. Hannah, W. B. *et al.* The expanding phenotype of *OFD1* -related disorders: Hemizygous loss-of-function variants in three patients with primary ciliary dyskinesia. *Mol Genet Genomic Med* **7**, (2019).

89. Meng, H. *et al.* The Relationship Between Human Papillomavirus, OFD1 and Primary Ciliogenesis in the Progression of Oropharyngeal Cancer: A Retrospective Cohort Study . *Pharmgenomics Pers Med* **Volume 13**, 633–644 (2020).
90. Kojima, R. *et al.* Abnormal accumulation of OFD1 in endometrial cancer with poor prognosis inhibits ciliogenesis. *Oncol Lett* **24**, 214 (2022).

Dottorando	**Dr.ssa Fabiola Piscopo**
Tutor	**Prof.ssa Brunella Franco**
Coordinatore	**Prof. Francesco Beguinot**
Corso di Dottorato in	**Dottorato di Ricerca in Medicina Clinica e Sperimentale**
Ciclo	**37°**
Codice borsa e n.	**DOT1318210-3 (Piscopo)**
CUP	**E65F21004010003**
Tipologia Green/Innovazione	**Innovazione**
Titolo Progetto	**Identificazione di nuovi biomarkers prognostici, predittivi e diagnostici nella medicina di precisione**

La borsa di dottorato è stata cofinanziata con risorse del Programma Operativo Nazionale Ricerca e Innovazione 2014-2020 (CCI 2014IT16M2OP005) risorse FSE REACT-EU, Azione IV.4 "Dottorati e contratti di ricerca su tematiche dell'innovazione" e Azione IV.5 "Dottorati su tematiche Green"